



## A Systematic Review of Synthesis MgO Nanoparticles and Their Applications

Hadia Hemmami<sup>1,2,3</sup> , Ilham Ben Amor<sup>1,2\*</sup> , Soumeia Zeghoud<sup>1,2</sup>, Salah Eddine Laouini<sup>1,4</sup>, Emmanuel Chile Nleonu<sup>5</sup> , Pawel Pohl<sup>6</sup> , Jesus Simal-Gandara<sup>7</sup> 

<sup>1</sup>Department of Process Engineering and Petrochemical, Faculty of Technology, University of El Oued, El Oued 39000, Algeria.

<sup>2</sup>Renewable Energy Development unit in Arid Zones (UDERZA), University of El Oued, El Oued 39000, Algeria.

<sup>3</sup>Laboratory of Applied Chemistry and Environment, Faculty of Exact Sciences, University of El Oued, P.O. Box 789, El Oued 39000, Algeria.

<sup>4</sup>Laboratory of Biotechnology Biomaterials and Condensed Materials, faculte de la technologie, , University of El Oued, P.O. Box 789, El Oued 39000, Algeria.

<sup>5</sup>Department of Chemistry, Federal Polytechnic Nekede, P.M.B. 1036, Owerri, Imo State, Nigeria.

<sup>6</sup>Department of Analytical Chemistry and Chemical Metallurgy, Faculty of Chemistry, University of Science and Technology, Wyspianskiego 27, 50-370 Wroclaw, Poland.

<sup>7</sup>Universidade de Vigo, Nutrition and Bromatology Group, Analytical Chemistry and Food Science Department, Faculty of Science, E32004 Ourense, Spain.

**Abstract:** Recently, nanoscale biotechnology has emerged as an essential field of contemporary science and a new era in the study of materials. It draws the attention of many scientists from all over the world due to its versatility in various fields. Many physical, chemical, and biological processes are used to create biomaterials. Among the materials of interest is magnesium oxide (MgO), which can be widely used in medical and biotechnological applications due to its non-toxicity and environmental friendliness. This review article discusses various methods for the synthesis of magnesium oxide nanoparticles (MgONPs), with particular emphasis on recent developments and applications of these nanomaterials.

**Keywords:** MgONPs, Synthesis techniques, applications.

**Submitted:** February 4, 2023. **Accepted:** February 28, 2024.

**Cite this:** Hemmami H, Ben Amor I, Zeghoud S, Laouini SE, Nleonu EC, Pohl, P, Simal-Gandara J. A Systematic Review of Synthesis MgO Nanoparticles and Their Applications. JOTCSA. 2024;11(2):731-50.

**DOI:** <https://doi.org/10.18596/jotcsa.1247385>

**\*Corresponding author's E-mail:** [ilhambenamor97@gmail.com](mailto:ilhambenamor97@gmail.com)

### 1. INTRODUCTION

Nanotechnology is a main driver behind the advancement of different disciplines of study that offers promise for numerous advances. Science and technology, deal with the synthesis, characterization, and development of applications of materials with at least one nanometer-scale dimension (1, 2).

Nanoparticles (NPs) are subgroups of particles with a size range of 1-100 nanometers that make up nanomaterials, which are structural components with a size range of 1-1000 nm (3, 4). Conical, spiral, flat, hollow, and other shapes and structures are just a few examples of the many different forms that can exist. Certainly, they exhibit exceptional physical

traits when compared to their bulk form, which gives them unique mechanical strength, improved stability, and many other advantages, and opens up the possibility for a range of unique applications (5, 6).

MgONPs are gaining more attention than other metal oxide nanoparticles that are frequently used in a variety of fields due to their high strength-to-weight ratio, low density, good functionality, nontoxicity, and hygroscopic properties. Because of their biocompatibility, they are very promising structural materials for implants and other biological systems. These characteristics of MgONPs boost their usefulness in several ways and provide additional benefits. It should not be surprising that MgONPs

have numerous commercial and biological applications in addition to their use in bone regeneration-assisting cryoinjury, antibacterial and antimicrobial inhibition, catalysis, lithium-ion battery production, and elimination of hazardous wastes (3, 7-11).

Because the synthesis method and its course determine the properties of the obtained nanomaterial and its subsequent use, the goal of this review study is to look into the methods involved in the synthesis of MgO NPs, with a particular emphasis on the most recent advancements in their various applications.

## 2. MAGNESIUM OXIDE NANOPARTICLE SYNTHESIS

Several methods are available for producing MgONPs, as shown in Figure 1. The most popular biological and chemical synthesis methods follow the bottom-up approach (12), and they are shown in Figure 1. Specifically, these methods include solve-/hydrothermal (13), sol-gel (14), co-precipitation (15), and combustion (16) processes. A special place among these methods is occupied using chemical reactions mediated by the use of plant extracts and microorganism media and fluids, the so-called green synthesis processes (17). In general, the bottom-up approach is advantageous because of its simplicity and ability to control the size and shape of the nanoparticles (18).

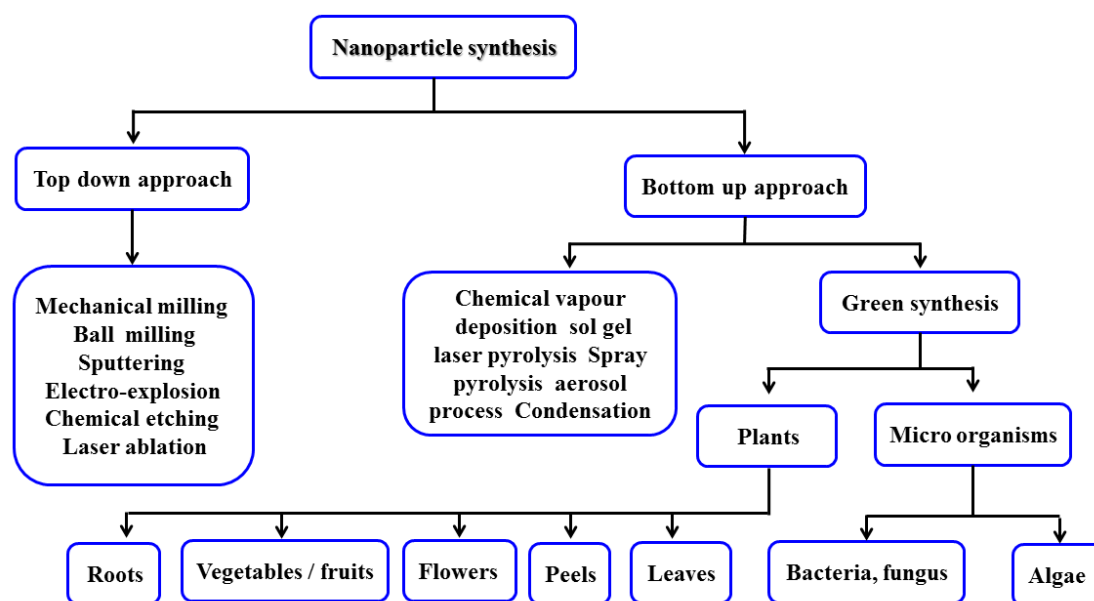


**Figure 1:** Different processes for creating nanoparticles.

### 2.1. Sol-Gel Technique

One of the simplest ways for synthesizing new material structures in the presence of an organic solvent and an inorganic precursor is the sol-gel method (19). Typically, this method is used to produce inorganic compounds like metal oxides and others that are comparable. In the middle of the 19th century, silica gel was first made using the sol-gel process (20). Metal alkoxides can be used to prepare homogeneous solutions, colloidal suspensions (sol), and integrated networks (gel), which, depending on the drying method, can subsequently be converted into xerogels or aerogels.

Mustuli *et al.* (21) focused on the production of nanostructured MgONPs using the sol-gel technique. They discovered that using Mg acetate in combination with a complexing agent in the form of oxalic acid and tartaric acid, the crystal growth could be inhibited.

Sutapa *et al.* (22) also produced MgONPs using Mg acetate. These researchers achieved the creation of cubic-shaped crystals, which were verified, using a scanning electron microscope (SEM), to have the highest texture coefficient value (0.98 in the crystal

plane (222)). They also characterized stress, strain, and crystal energy.

Wahab *et al.* (23), synthesized MgONPs using  $\text{Mg}(\text{NO}_3)_2$  and NaOH. The sol-gel method described in their work resulted in the production of cubic-shaped MgONPs with a size of 50-60 nm.

In contrast, using Mg ribbons as a precursor, Boddu *et al.* (24) documented the synthesis of MgONPs having a coralline structure. In this case, hydrolysis, supercritical drying, and heat activation processes were carried out after a solution of Mg methoxide was obtained. This applied method resulted in the fabrication of 200–300 nm-sized particles having the aforementioned structure. To produce a nanopowder from MgO xerogel, Mg methoxide was employed by Dercz *et al.* (25) as a precursor, and the hydrolysis in the presence of toluene, followed by the addition of methanol was carried out. In this way, a specific surface area of  $138 \text{ m}^2/\text{g}$  and an average crystallite size of 7.5 nm were attained for these MgONPs.

Rani *et al.* (26) employed  $\text{Mg}(\text{NO}_3)_2$ , which dissolved in distilled water. SEM examinations showed that the final particles, produced *via* gel grinding and

subsequent annealing, had an average size of 60 nm. Nassar *et al.* (27) employed a mixed sol-gel combustion technique to produce nanostructured MgONPs as well. The scientists discovered that the kind of fuel had no discernible impact on the size and shape of the crystallites when utilizing  $\text{Mg}(\text{NO}_3)_2$  in combination with oxalic acid, urea, and citric acid (citric acid was used to create the lowest crystallite size, which was about 12 nm).

## 2.2. Co-Precipitation

The synthesis of NPs with this method is based on the idea of precipitation, and frequently uses liquid-phase synthesis (28), while vapor-phase synthesis is applied less frequently (29). The precipitating agent is frequently NaOH (30, 31), and two processes, i.e., nucleation and nuclei growth, make up together the homogeneity of the precipitation reaction and the quality of the final nanomaterial product (32). Three basic concepts are taken into account: (i) the diffusion-based single nucleation and the homogeneous growth; (ii) the smaller subunits formation, development, and assemblage; and (iii) the numerous nucleation and the Ostwald ripening growth (33).

Mashad *et al.* (34) produced MgONPs by co-precipitation and evaluated the effects of various reaction parameters, such as temperature, pH, and the molar ratio of precursor (magnesium nitrate), on the quality of the products. They obtained nanoparticles and nanorods with a reasonably high specific surface area (231  $\text{m}^2/\text{g}$  for nanoparticles and 176  $\text{m}^2/\text{g}$  for nanorods) and a particle size of 50 nm.

$\text{Mg}(\text{NO}_3)_2$  was used as the precursor, while an  $\text{NH}_4\text{OH}$  solution served as the precipitating agent in work by Kumar *et al.* (35). As a result, MgONPs having an average size of around 11 nm were produced. The impact of the polyethylene glycol (PEG) content on the characteristics of MgONPs produced by the co-precipitation method was also investigated by Karthikeyan *et al.* (36). In this work,  $\text{Mg}(\text{NO}_3)_2$  was used as a precursor while NaOH as a precipitation agent. When PEG was additionally used, it resulted in doubling the size of crystallites, according to XRD measurements (8.6 nm vs. 14.8–15.9 nm without and with PEG, respectively). What is more, PEG-modified MgONPs exhibited a flake-like structure, while pure MgONPs were spherical.

By calcining  $\text{MgCO}_3$ , which Frantina *et al.* (37) initially obtained by combining  $(\text{NH}_4)_2\text{CO}_3$  and  $\text{MgCl}_2$ , MgONPs were also produced. The XRD data suggested a cubic structure with an average crystallite size of 24 nm. With negligible changes in the particle size, the spherical shape of the resulting MgONPs was confirmed using SEM, while their average size was 50.9 nm.

MgONPs reported by Kushwaha *et al.* (38) were produced by several distinct techniques (sol-gel, solution combustion, and a solution of cetyltrimethylammonium bromide (CTAB)), as well as the co-precipitation technique. Their findings demonstrated that 4.9 eV bandgap MgONPs were produced using the chemical method. The crystallite

size was shown by XRD to be 14.8 nm, and the authors also reported a hydrodynamic particle size of 100 nm. MgO nanotubes were also prepared by Tandon and Chauhan (32) using Mg acetate and NaOH. Using XRD, the average crystal size was calculated to be 34 nm. The field emission (FE)SEM data showed that the resulting nanomaterial had a tubular shape, with an inner diameter of 31 nm and an estimated outside diameter of 78 nm. Additionally, a greater bandgap of MgONPs in comparison to the prior example (5.73 eV) was reported.

## 2.3. Combustion Technique

Due to its effectiveness and affordability, the combustion process is commonly utilized to manufacture metal oxide nanoparticles (39). Two strategies can be used for that, including so-called "self-propagating synthesis" and the "volume combustion synthesis" (40). In the case of "self-propagating synthesis", the production of solid products occurs without the need for the energy input (41), because spontaneous redox reactions occur between the precursor (oxidizer) and the reductant (fuel) combined at the molecular level in solution. These reactions are initiated by an outside source. In the second case ("volume combustion synthesis"), the sample is heated until the reaction starts, spreading across its whole volume. The latter approach is especially recommended for moderate exothermic reactions that require preheating before the ignition, even though this sort of preparation is more difficult to control (42).

Accordingly, when urea was used as a fuel and  $\text{Mg}(\text{NO}_3)_2$  as an oxidizer, it was possible to produce MgONPs with a cubic structure and a crystallite size of around 22 nm, according to the XRD data (43). The resulting MgONPs were uniformly sized and spherical, as established by SEM. Interestingly, the synthesized nanomaterial exhibited a bandgap of just 2.9 eV, which is much lower as compared to earlier research. The same raw ingredients were utilized by Rao *et al.* (44), who tested the impact of the fuel-to-oxidizer ratio on the quality of the produced nanomaterial. The findings showed that except for the percentage of oxidizer was 0.75, manufactured MgONPs have larger crystallite sizes (18–53 nm) when the fuel contribution increases. Changes in the burn rate, enthalpy, or ignition temperature might be responsible for this.

Ranjan *et al.* (45) reported a variation of this procedure, using  $\text{Mg}(\text{NO}_3)_2$  as the precursor and glycine as the fuel. The estimated crystallite size, based on the XRD measurements, was 20.8 nm in this case.

On the other hand, Therami *et al.* (46) used citric acid as fuel. The authors examined how the specified parameters of MgONPs were impacted by the concentration of this acid. The most significant changes obtained were observed for the particle size of MgONPs (it decreased from 35 to 20 nm), their bandgap (it increased from 4.72 to 5.35 eV), and their morphology (vacuolar, flower-like, and flake-like).

MgONPs were also obtained by Kumar *et al.* (47), who used  $\text{Mg}(\text{NO}_3)_2$  and a parthenium plant extract. The primary objective was to analyze the impact of the fuel quantity on the bandgap width (5.3–5.45 eV) and the crystallite size (27–35 nm). However, the variation of both parameters was not as pronounced as it was reported in other works.

#### 2.4. Solvo- and Hydrothermal Method

Another popular technique for regulating the formation of crystals in a variety of materials is the solvothermal approach (48). The required products are generated when a precursor and a suitable solvent are put in an autoclave and exposed simultaneously to a high temperature and a high pressure (49). In contrast to the co-precipitation approach, these reaction conditions (temperature and pressure) enable to obtain the high crystallinity materials (50). Solvents other than water are typically utilized in the "solvothermal" technique, including alcohols or other organic or inorganic solvents. When water is used as the solvent, this process can be referred to as "hydrothermal."

Devaraja *et al.* (51) used  $\text{Mg}(\text{NO}_3)_2$  and NaOH to produce a nanocrystalline MgO powder and evaluated its quality. The MgONPs produced by them were porous, with an average crystallite size of 25 nm and an optical energy bandgap of 5.5 eV. Al-Hazmi *et al.* (52), on the other hand, obtained nanofibers by the direct interaction of urea and Mg acetate. These fibers had an average crystallite size of 6 nm, which corresponded to their diameter, and the length of 10 nm, as measured by TEM.

Ding *et al.* reported the synthesis of rod- and tube-shaped  $\text{Mg}(\text{OH})_2$ , which was subjected to thermal decomposition to fabricate MgONPs (53). The author's findings demonstrated that the hydrothermal approach could be used to manipulate the crystallite size of the resultant MgONPs, and their shape and structure. The material for the synthesis was either Mg powder,  $\text{Mg}(\text{SO}_4)_2$ , or  $\text{Mg}(\text{NO}_3)_2$ . Due to various experimental circumstances, numerous morphologies (lamellar, needle-like, and rod-like) of MgONPs were achieved. The resultant nanomaterials were 20 to 600 nm in size and had a specific surface area of more than 100  $\text{m}^2/\text{g}$ .

Rukh *et al.* (54) used Mg powder as the precursor for the MgONPs synthesis. The reaction medium for the synthesis was a mixture of  $\text{H}_2\text{O}_2$  and de-ionized water. Using this method, MgONPs with an 18 nm crystallite size were obtained. Nanoplates are another form of nanostructured MgO that was reported to be produced by Duong *et al.* (54). Additionally, the scientists utilized sodium dodecyl sulfate (SDS), PEG, CTAB, and  $\text{Mg}(\text{NO}_3)_2$  to regulate the morphology of the resulting nanomaterials. MgONPs produced using the hydrothermal process in conjunction with SDS were the most intriguing since they had the largest specific surface area (126  $\text{m}^2/\text{g}$ ) and the ideal disc shape (thickness 5 nm, diameter 40–60 nm).

#### 2.5. Green Synthesis of MgO Nanoparticles

Researchers have shown a growing interest in the production of MgONPs through biological processes over the past ten years. The development and significance of this synthesis type are mostly related to the possibility of the use of much fewer chemicals, making this less cost-effective and more environmentally friendly (55–57).

The traditional chemically- or physically-based techniques for the synthesis of MgONPs are less practical and less ecologically benign than their biologically-based alternatives, also known as (56, 58). Consequently, the term "green synthesis" is frequently used to describe biological techniques. The large-scale synthesis of nanoparticles utilizing the green methods is always a difficult undertaking, and these are only performed at laboratory-scale processes. However, thanks to advancements in the understanding of the nature of the biological extract composition and the reaction with metal ions, large-scale preparation may soon be feasible without the need for any powerful machines (59).

To lessen the hazardous nature of the nanoproductions, biological substrates such as plants, bacteria, algae, and fungi are frequently utilized in place of chemical compounds used as stabilizers and solvents (59). The greener way to produce MgONPs involved the use of the available precursors, such as  $\text{Mg}(\text{NO}_3)_2$ ,  $\text{MgCl}_2$ , Mg acetate, and  $\text{Mg}(\text{SO}_4)_2$ , and different biological agents, including plants, microorganisms, and biomolecules. The precursor was combined with the previously produced biological extracts of plants, microorganisms, or templates to prepare homogeneous mixtures, which were then subjected to thermal treatment (60–62).

There are several papers on the production of MgONPs. The information on the various synthetic processes used to produce nanostructured MgO reported in the literature is given in Table 2. Many biological templates were employed for the production of MgONPs, as can be seen from the data given. The production of MgONPs with various sizes and morphologies was ultimately achieved by the variation in the reaction time, the concentration of the Mg precursors, pH, and the temperature of the reactants.

For instance, it was established that the particle size of MgONPs grows along with the increasing dose of the biological substrate (63). According to the Mie hypothesis, the absorbance of light is proportional to the particle size of the metal nanoparticles formed. However, it was discovered (64) that when the extract of *Amaranthus tricolor* and Mg acetates ( $\text{Mg}(\text{C}_2\text{H}_3\text{O}_2)_2$ ) were used, the MgONPs produced were found to deviate from the Mie theory, showing the lower absorbance and the increased particle size when the amount of the biological substrate was higher. When they added 5 mL of the *Amaranthus tricolor* extract and Mg acetate, they found that the product had a little variation from the Mie theory; it had decreased absorbance and increased particle size. Smaller-sized MgONPs resulted from the addition of 10 and 15 mL of the *Amaranthus tricolor*

extract to the same precursor. This demonstrated how the presence of the biological substrates affects the size of MgONPs. According to scientists, the addition of capping agents could also improve the production of MgONPs. Smaller amounts of the capping agents caused the particles to adhere to one another and, to larger extents, the formation of larger particles. It is also obvious that the use of lower concentrations of the biological substrates would produce more homogeneous and bigger nanoparticles, whereas higher concentrations of the biological substrates would produce less stable nanoparticles. It is also evident that the presence of flavanoids in the biological substrates is responsible for these modifications. The development of MgO NPs is also influenced by reaction time. Additionally, the size of the product rises along with the response time. Numerous pH reports at 3.2, 5.2, 7.2, and 9.2 are available. It is clear from examining the impact of pH reports that a pH of 3.2 results in good particle size. The biological templates' active components, like flavonoids and polyphenols, are particularly effective at reducing metal ions at this pH level (65).

Khan *et al.* (66) noticed that the temperature also has an impact on the formation of MgONPs. The authors conducted the reaction at temperatures between 30 and 70 °C while holding all other variables constant. Generally speaking, the appropriate temperature should be kept for the formation of MgONPs with phytochemical support (Flavonoids, phenols, and other species). Otherwise, the phytochemicals utilized to synthesize MgONPs could alter their structure. The highest absorbance (81%) range of methylene blue (MB) dye was achieved at 30 °C. Additionally, it was noticed that when the temperature was raised, product agglomeration occurred, while product formation was prevented. Furthermore, the production of the final product was hampered by precursor concentrations greater than 0.001 mol/L. The final loss of chemicals, energy, and time will occur from the addition of an excessive concentration of the precursors. The physicochemical properties of MgONPs can be altered depending on the conditions of the green synthesis conditions (see details in Table 2).

**Table 1:** Individual ingredients and reaction circumstances for the bottom-up production of nanostructural MgO using various techniques.

Sol-Gel Technique							
Precursor	Solvent(s)	Drying temperature (°C)	Temperature of calcination (°C)	Time of calcination (h)	Size (nm)	Expected applications	Ref.
Mg(NO <sub>3</sub> ) <sub>2</sub>	C <sub>6</sub> H <sub>8</sub> O <sub>7</sub> , C <sub>2</sub> H <sub>2</sub> O <sub>4</sub> , NH <sub>2</sub> CONH <sub>2</sub>	350	550, 800	2	12	catalyst	(27)
Mg(CH <sub>3</sub> COO) <sub>2</sub>	C <sub>4</sub> H <sub>6</sub> O <sub>6</sub> , NaOH	-	600	6	-	-	(21)
Mg(CH <sub>3</sub> COO) <sub>2</sub>	C <sub>2</sub> H <sub>2</sub> O <sub>4</sub>	200	950	6	-	-	(22)
Mg(NO <sub>3</sub> ) <sub>2</sub>	NaOH	300	500	2	50-60	adsorber	(23)
Mg(OCH <sub>3</sub> ) <sub>2</sub>	CH <sub>3</sub> OH, C <sub>7</sub> H <sub>8</sub>	-	500	5	200-300	-	(24)
Mg(OCH <sub>3</sub> ) <sub>2</sub>	CH <sub>3</sub> OH; C <sub>7</sub> H <sub>8</sub>	60	450	-	Ca.8	-	(25)
Mg(NO <sub>3</sub> ) <sub>2</sub>	H <sub>2</sub> O	150	500	2	60	-	(26)
Co-Precipitation Technique							
Precursor	Precipitation agent	Reaction temperature (°C)	Temperature of calcination (°C)	Time of calcination (h)	Size (nm)	Expected applications	Ref.
Mg(NO <sub>3</sub> ) <sub>2</sub>	NaOH	Room	Room	-	78	antibacterial agent	(32)
Mg(NO <sub>3</sub> ) <sub>2</sub>	NaOH	-	440	4.5	-	catalyst	(38)
Mg(NO <sub>3</sub> ) <sub>2</sub>	NH <sub>4</sub> OH	60, 70, 80	550	2	50	-	(34)
Mg(NO <sub>3</sub> ) <sub>2</sub>	NH <sub>4</sub> OH	100	600	4-6	11	antibacterial agent	(35)
Mg(NO <sub>3</sub> ) <sub>2</sub>	NaOH	Room	500	4	14-16	antibacterial agent	(36)
Combustion Technique							
Oxidizer	Fuel	Ignition temperature	Temperature of calcination (°C)	Time of calcination (h)	Size (nm)	Expected applications	Ref.
Mg(NO <sub>3</sub> ) <sub>2</sub>	Parthenium extract	400	-	-	27-35	photocatalyst	(47)
		70-80	500	3	22	adsorber	(43)
	NH <sub>2</sub> CONH <sub>2</sub>	100	300	2	18-53	-	(44)
	NH <sub>2</sub> CH <sub>2</sub> COOH	170	600	2	Ca.21	fuel additive	(45)
	C <sub>6</sub> H <sub>8</sub> O <sub>7</sub>	100	400	15 min	20-35	antibacterial agent	(46)
Solvo- and Hydrothermal Technique							
Oxidizer	Solvent	Autoclave temperature	Temperature of calcination (°C)	Time of calcination (h)	Size (nm)	Expected applications	Ref.
Mg(NO <sub>3</sub> ) <sub>2</sub>	NaOH	100	500	4	40-60	adsorber	(67)
Mg	H <sub>2</sub> O <sub>2</sub>	220	-	-	18	antibacterial	(54)
MgSO <sub>4</sub>	NH <sub>3</sub> H <sub>2</sub> O; en-H <sub>2</sub> O	180	280-450	1;2	100-200	catalyst	(53)

Mg(NO <sub>3</sub> ) <sub>2</sub>	NaOH	130	400-800	2	25	-	(51)
Mg(CH <sub>3</sub> COO)	NH <sub>2</sub> CONH <sub>2</sub>	180	600	1	6	antibacterial	(52)
Mg(NO <sub>3</sub> ) <sub>2</sub>	NaOH	80	280-450	1;2	50	catalyst	(53)
Green Synthesis							
Precursor solution	Reagent extract	Reaction temperature	Temperature of calcination (°C)	Time of calcination (h)	Size (nm)	Expected applications	Ref.
Mg(NO <sub>3</sub> ) <sub>2</sub>	<i>Nephelium lappaceum</i>	80	450	-	55	-	(68)
	<i>Trigonella foenum-graecum</i>	80	600	4	14	antibacterial agent	(69)
	<i>Rosa foribunda</i>	90	-	-	10	antibacterial agent	(70)
Bulk MgO	<i>Rosmarinus officinalis</i>	70	-	-	8.8	antibacterial agent	(71)
Mg(NO <sub>3</sub> ) <sub>2</sub>	<i>Dalbergia sissoo</i>	30-70	-	-	50	photocatalyst	(66)
	<i>Saussurea costus</i>	80	450	3	30	photocatalyst	(72)
	<i>Swertia chirayaita</i>	55	400	4	< 20	antibacterial agent	(73)
MgCl <sub>2</sub>	<i>Moringa oleifera</i>	90	600	5	21	antibacterial agent	(74)
Mg(NO <sub>3</sub> ) <sub>2</sub>	<i>Tecoma stans</i>	90	550	6	20-50	adsorber	(75)

**Table 2:** Reported processes for making MgO NPs through green synthesis.

Material used	Particle size (nm)	Morphology of nanomaterial	Activity carried	Ref.
<i>Citrus limon</i> leaf extract	12-80	nanoflakes	nil	(58)
<i>Rosmarinus officinalis</i>	<20	nanoflowers	antibacterial activity	(71)
<i>Nephelium lappaceum</i>	60-70	cubic	nil	(76)
<i>Solanum trilobatum</i>	30 and 42	spherical	antibacterial and antioxidant activity	(77)
<i>Mucuna pruriens</i> seeds	35	spherical	antibacterial and photocatalytic activity	(78)
<i>Rhizophora lamarckii</i>	20 and 50	hexagonal and spherical	antibacterial activity	(79)
<i>Aloe vera</i>	8.6	dense rock-shaped flakes	antibacterial and photocatalytic activity	(80)
<i>Amaranthus blitum</i> and <i>aloe vera</i>	26-50	spherical	water treatment	(81)
Mushroom extract	20-15	cubic	seed germination	(82)
<i>Aspergillus tubingensis</i>	2.8	sphere	nil	(83)
<i>Aspergillus niger</i>	43-91	sphere	antibacterial activity	(84)
<i>Lactobacillus plantarum</i>	30	cubic	anticancer activity	(85)
<i>Lactobacillus sporogenes</i>				
<i>Aspergillus fumigatus</i>	0.3-94	nil	nil	(86)
<i>Manihot esculenta</i>	37	hexagonal	nil	(87)
<i>Sargassum wightii</i>	69	cubic	antimicrobial and photocatalytic activity	(88)
<i>Artemisia abrotanum</i> herb	10	clusters	photocatalytic and antioxidant activity	(89)
<i>Rhododendron arboretum</i>	nil	nil	antibacterial activity	(62)
<i>Ocimum sanctum</i>	50-100	nanoflakes	antibacterial and antioxidant activity	(81)
<i>Chamaemelum nobile</i> flower extract	20-40	nanoflakes	insect repellent	(90)
<i>Curcumin</i>	35	rod-like and spherical - like shape	catalytic properties	(91)
<i>Acacia</i> gum	50-78	nanoflowers, cubic	catalytic properties	(92)
<i>Brassica oleracea</i> and <i>Punica granatum</i>	30-65	spherical	photocatalytic and anticancer activity	(93)

Orange peel extract	>10	spherical	antibacterial and antimicrobial activity	(94)
Curry leaves	20	spherical	photocatalytic activity	(95)
<i>Swertia chirayaita</i>	<20	spherical	antibacterial activity	(73)
<i>Pisidium guvajava</i> and <i>aloe vera</i>	50-90	cubic	antibacterial activity	(96)
<i>Lepidium sativum</i>	33	nanoflakes	photocatalytic activity	(97)
<i>Matricaria chamomilla</i> L. extract	18 and 16	disc-shape	antibacterial activity	(98)

### 3. RESOURCES THAT CAN BE USED AS A MAGNESIUM SOURCE TO PREPARE MgO NPs

MgO nanoparticles with superior properties are important in industry, and these particles can be prepared from different sources using different methods. Table 3 shows the resources that can be

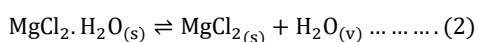
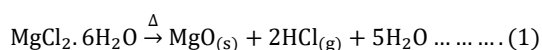
used to manufacture MgO NPs as a source of magnesium in a direct way. As for the indirect method, an intermediate is extracted and subsequently treated to produce magnesium oxide (Table 4). The following chemical equations (1-4) explain the mechanism of transformation of the medium into magnesium oxides.

**Table 3:** There are several resources that may be employed to manufacture MgO NPs as a magnesium source.

Resources	Presses	Intermediate reactant	Temperature of calcination (°C)	Yield%	Purity%	Size (nm)	Ref.
Dolomite CaMg(CO <sub>3</sub> ) <sub>2</sub>	Pyrohydrolysis process	HCl CO <sub>2</sub>	600	98.10	98.86	100	(99)
Dolomite: CaMg(CO <sub>3</sub> ) <sub>2</sub> ]	Pyrohydrolysis process	HCl MgCl <sub>2</sub>	500	--	95.48	--	(100)
Dolime (CaO.MgO)	Pyrohydrolysis process			--	87.80	--	
Serpentine;		(NH <sub>4</sub> ) <sub>2</sub> SO <sub>4</sub> NaHSO <sub>4</sub>	1300	--	high purity	62	(101)
Dolomite : poly(acrylate) magnesium hydroxide	Pyrohydrolysis process	poly(acrylate) Na <sub>2</sub> S <sub>2</sub> O <sub>8</sub> MgCl <sub>2</sub> NaOH	500	--	high purity	20	(102)
Sea water	Pyrohydrolysis process	MgCl <sub>2</sub> NaOH	1400	43	56	--	(103)

**Table 4:** Various resources that may be employed to prepare an intermediate reactant using a magnesium source.

Resources	Technique	Reactants	Temperature of reaction (°C)	Yield %	Purity %	Size (nm)	Ref.
serpentine mineral	precipitation	NH <sub>4</sub> OH HNO <sub>3</sub>	80	--	high purity	30	(104)
Serpentine 4MgCO <sub>3</sub> .Mg(OH) <sub>2</sub> . 4H <sub>2</sub> O	precipitation	NH <sub>3</sub> .H <sub>2</sub> O NH <sub>4</sub> HCO <sub>3</sub>	40~70	96.3	high purity	--	(105)



mode. Mono-coordinated hydroxyl (-OH) groups are indicated at 3100–3500 cm<sup>-1</sup>. The stretching frequency of H-O-H is linked to a wide band at roughly 3461 cm<sup>-1</sup>. At roughly 673 cm<sup>-1</sup>, the wide band stretching vibration matches the Mg-O stretching vibration. The stretching vibration of magnesium oxide is shown by a prominent peak with a center of 433–769 cm<sup>-1</sup>.

### 4. CHARACTERISTICS MgO NPs

Magnesium oxide may also be identified and structurally characterized using Fourier transform infrared spectroscopy (FTIR)(106, 107). Depending on the wavelength of the incoming light, transmittance or absorbance are the most typical interpretations. Figure 2a displays typical FTIR spectra for magnesium oxide in the absorbance

Using X-ray diffraction (XRD) (JCPDS Standard No. 01-089-7746), it is possible to characterize the crystal structure of magnesium oxide. Important peaks can be assigned near the 2θ values of 36.8, 42.9, 62.19, 74.6, and 78.58°, which can be indexed to the lattice planes (111), (200), (220), (311), and (222), respectively. Comparable findings have been frequently reported(108) (Figure 2b). The most

popular method in the literature for interpreting XRD data to calculate the crystallite size of produced nanostructures is the Scherrer equation(109). Nevertheless, the average crystallinity size up to around 200 nm(110) is the limiting factor in terms of employing the Scherrer equation. This is caused by the fact that when crystallite size increases, the diffraction peak's widening reduces(111). Hence, it is challenging to distinguish between the widening of the peak caused by crystallite size and the

broadening caused by other causes (e.g., size distributions and shape of the crystallites)(106).

In addition to the methods mentioned above, UV-Vis spectroscopy (UV-Vis) and spectra are taken between 200 nm and 800 nm. They may also be used to analyze MgO, especially to establish the bandgap energy(112, 113). Tauc plots and absorbance spectra are both utilized for this. To measure the bandgap width, the photoluminescence technique(114) is usually employed.

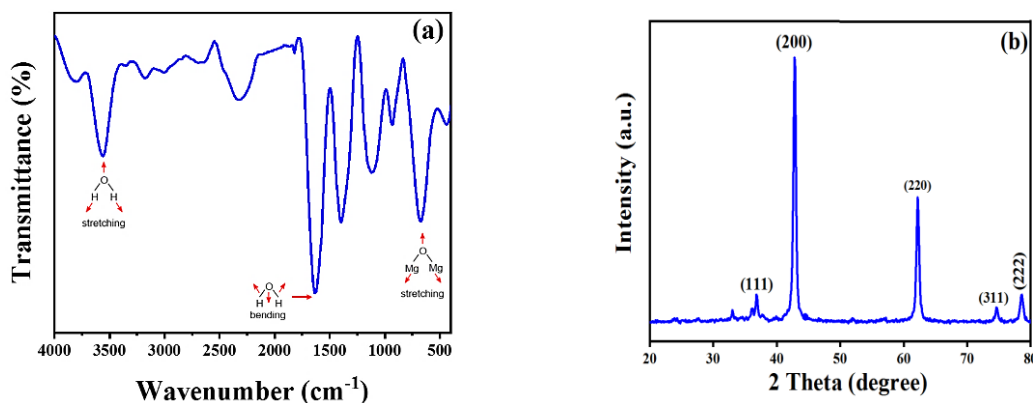


**Figure 2:** FTIR spectra (a) and an XRD pattern(b) used to characterize the structural properties of MgONPs (redrawn and adapted from the results presented in(115)).

Depending on several variables, including the synthesis process, the synthesis circumstances, and the post-treatment techniques, MgO structures can have a variety of morphologies. Typical morphological variations between MgO formations include the following:

**Particle size and shape:** The synthesis technique utilized can have a significant impact on the size and form of MgO particles. For instance, sol-gel processes may yield a range of morphologies, including nanowires and sheets, whereas precipitation methods usually produce spherical particles with a restricted size distribution(116).

**Surface area:** Depending on their form, MgO structures' surface areas can also change. Larger particles often have lower surface areas than nanoparticles or nanowires, which might be crucial for applications like catalysis(117).

**Porosity:** Depending on the synthesis technique employed, MgO structures can be either very porous

or non-porous. For instance, although hydrothermal synthesis may yield structures with a high degree of crystallinity and little porosity, flame synthesis can produce very porous structures, such as hollow spheres(118).

**Crystal structure:** The crystal formations of MgO can be cubic, hexagonal, or tetragonal. The material's chemical and physical characteristics can be affected by the crystal structure(119).

**Surface chemistry:** Depending on their form, MgO structures' surfaces can have different chemical compositions. For instance, exposed crystal planes or surface flaws might influence the reactivity of MgO in catalytic processes(120).

The morphology and properties of the prepared MgONPs differ and depend on the synthesis route and processing conditions. Figure 3 illustrates the various morphologies that can be seen in MgO nanoparticles.

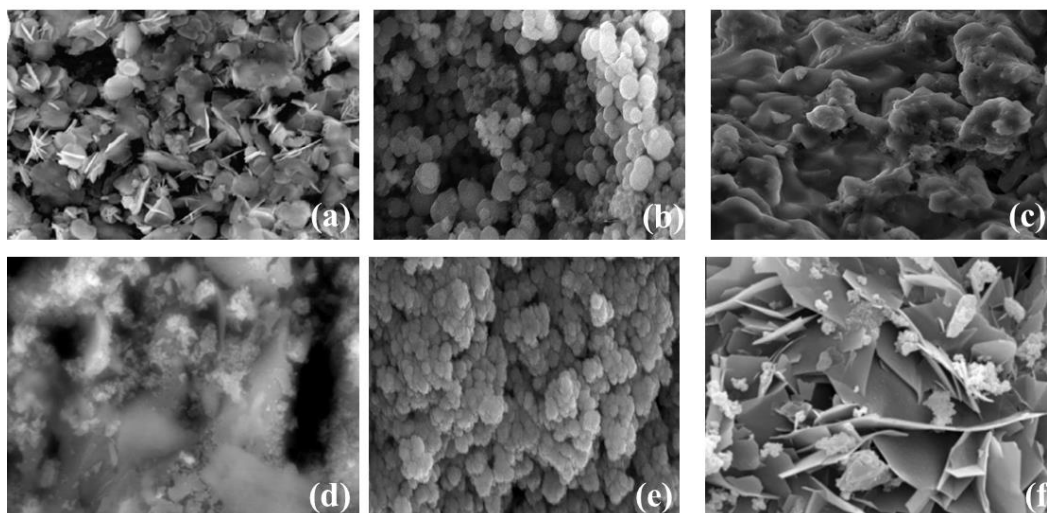


**Figure 3.** Different morphologies of MgO NPs: (a) flower-like(121), (b) spherical(115),(c) irregular shaped flakes(97),(d) Clusters(122),(e) Hexagonal(87),(f) flakes shape(87).

## 5. APPLICATIONS

MgONPs have a large specific area, a broadband gap, and good physical and chemical properties, providing them with strong technological applications. Additionally, MgONPs exhibit a propensity to generate superoxides when they are in contact with  $O_2$  found in bacterial cell walls. The bacterial cell walls

and their phospholipids are promptly destroyed by these superoxides, which are highly responsive to them. MgONPs can also be used in many applications, as displayed in Figure 4, including the production and/or modification of fuel cells, ceramics, batteries, supercapacitors, and electronics, in addition to environment and agriculture purposes.

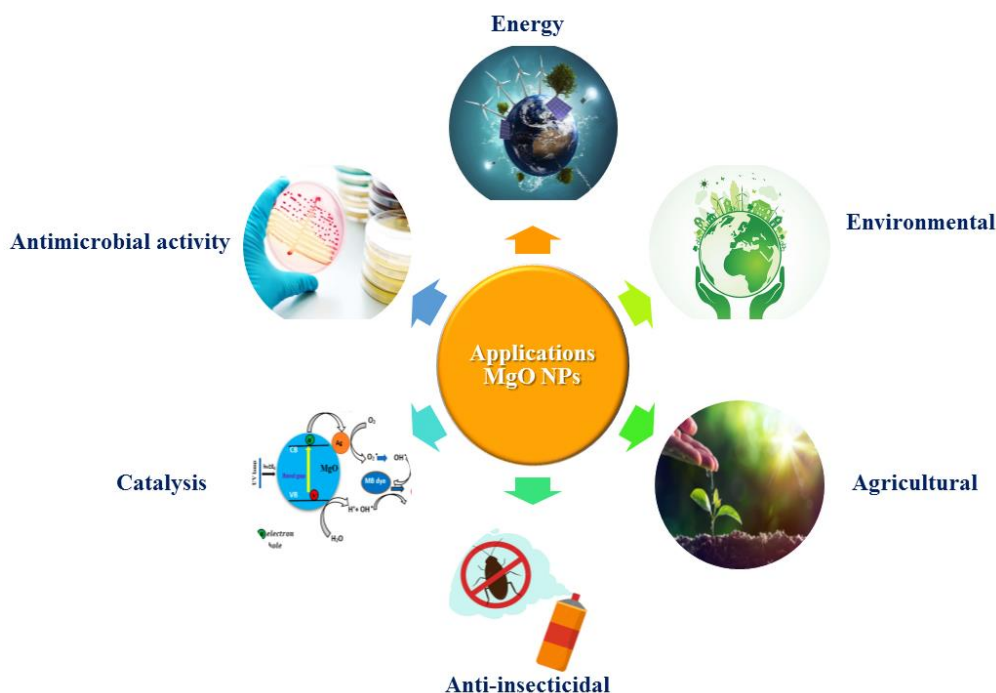


**Figure 4:** Different applications of MgONPs.

### 5.1. Energy

Recently, the global world has seen a surge in air pollution, global warming, and sea level rise as a result of the depletion of fossil fuels. Therefore, it is critical to locate a substitute for these changes. Fuel cells, solar cells, and batteries as fossil fuel alternatives could be a very good remedy. In addition to the production of  $H_2$ , which is a good fuel and a superior substitute for carbon-based bi-products, they will also release water as a byproduct. Magnesium performs better than other metals in the storage of  $H_2$ . The storage of  $H_2$  is stated to benefit

from the use of chemical hydrides such  $NaAlH_4$ ,  $LiBH_4$ , and  $LiNH_2$  as well as metal hydrides like  $Pd@H$ ,  $V@H$ , alloys like  $TiFeH_2$ ,  $LaNi_5H_6$ ,  $Ti@V@Mn@H$ ,  $Mg_2NiH_4$ , and certain complicated hydrides. Compared to the other hydrides, Mg has the benefit of being extremely abundant in the earth's crust, having a higher capacity to store  $H_2$ , and having an ecologically benign and cost-effective nature (123). There are numerous reports of these MgO-based batteries that use polymers (124), pigments like acetylene black (125), metals like Na (126), Li, V (127), carbon substrates (128), and B. These energy

storage technologies are reliable, safe, affordable, and ecologically benign.

### 5.2. Catalysis

MgONPs are also frequently used in heterogeneous catalysis for several chemical reactions, including the oxidative coupling of CH<sub>4</sub>, the dehydration of alcohols, the benzylation of aromatics, the dehydrohalogenation of halogenated hydrocarbons, the production of pyranopyrazole and its derivatives, the benzylation of aromatics, the dehydrohalogenation of halogenated hydrocarbons. In this case, nano-structured MgO is utilized as a support for catalysts due to its structure, basicity, and electronic and electrochemical properties, making it easier to move the electrons across the catalyst surface (129, 130). Vegetable oils were recently trans-esterified using MgO as a catalyst (131). Other reactions, *i.e.*, Wittig (132), Cyanosilylation (81), Aldol (133), Mannich (134), aza-Michael (135), Baylis-Hillman (136, 137), were

also catalyzed with the aid of MgONPs. The enormous surface area and the distinctive morphology of MgO are thought to be the cause of its observed high catalytic activity (138).

### 5.3. Agricultures

MgONPs are also known to offer several benefits, including low phytotoxicity, non-genotoxicity, and non-biotoxicity to people, and thermal stability, which open up a wide range of potential applications of this nanomaterial for plant protection (139). Along with the aforementioned qualities, MgONPs also possess several additional traits that make them particularly useful in a variety of different agricultural applications, as illustrated in Figure 5 (140). Additionally, these nanoparticles aid in the development of seedling and plant growth and are utilized as an authorized food supplement, a food additive, a color retentate, and also in increasing the agricultural production of peanuts (141, 142).



**Figure 5:** Potential applications for MgO NPs in the agricultural domain.

### 5.4. Biomedical

Because of their high absorption capability, high reaction activity, active catalysis property, and enzyme immobilization, MgONPs are used in the development of the diagnosis of cancer and the guidance of the cure plan through medical imaging. For use in dentistry, surgery, bacterial suppression, tissue engineering, and bone mending, bioactive glass is currently being developed (143, 144). Research findings support the addition of MgONPs to several medicinally valuable chemicals due to their various qualities, including antibacterial, anticancer, biocompatibility, nontoxicity, and cheap cost. MgO also seems to have several safe and useful medicinal applications. Given the potential for negative impacts from exposure to MgONPs, we must have the best method to both reap the benefits of MgONPs and prevent any negative effects that may arise (145).

### 5.5. Anti-microbial Activity

By inducing a breach in their cell membrane and eventually resulting in their death, MgO NPs have antibacterial action against food-borne pathogens such as *E. coli* and *Salmonella enteritidis* (146). The bacterial strain *Acidovorax oryzae* is the source of the illness known as the bacterial brown stripe, which is known to spread among rice and entirely ruin rice farming. As a result, Ogunyemi *et al.* reported on the biosynthesis of MgO NPs utilizing *Matricaria chamomilla L.*, which showed a good inhibitory impact on the development of *Acidovorax oryzae* bacteria (98). The worst wilt disease in *R. solanacearum* is caused by phytopathogenic bacteria, which were found to have a favorable antibacterial response to MgO NPs in another study (147). Accordingly, MgO NP nanoflowers were also developed because they possess the ability to inhibit bacterial infections and shield crops from harmful attacks (148). Due to the role of Mg in the

pathogenesis, plant defense, and other physiological processes, as well as the importance of this metal for maintaining balanced nutrition in plants, MgO NPs are known to have a strong antifungal action even at low fungicidal concentrations (149-152).

### 5.6. Anti-biofilm Activity and Anti-insecticidal

Cry genes are proteins produced by *Bacillus thuringiensis* that function as an insecticide against a variety of insects, including nematodes. However, this protein is released into the soil by water, which hinders its insecticidal effectiveness. By adhering this protein to MgO NPs and subsequently transferring them to the surface of cotton leaves, Rao *et al.* (153) indicated increased insect fatality rates across the board. As a result, cry protein was transferred *via* MgO NPs, which enhanced their use as bioinsecticides (154). By limiting the development of the biofilms, MgO NPs are known to promote systemic resistance against the gram-negative, plant-pathogenic bacterium *R. solanacearum*. They can also start the signaling of pathways for phytohormones like jasmonic acid and salicylic acid, which are crucial components of the plant's defense mechanisms. Therefore, it should be noted that MgONPs are highly efficient anti-microbial, antibiofilm agents, and anti-insecticidal in agricultural fields (155, 156).

### 5.7. Environmental

The major issue of environmental pollution affects both developed and developing countries worldwide. There are several ways to deal with this global problem, but one downside is that certain cleaning chemicals have side effects that make them act as contaminants themselves. Nanoparticles appear to be a fantastic replacement for several various environmental applications (Figure 4). MgONPs are effective in a variety of environmental remediation. These metal oxide NPs are utilized as a possible adsorber of harmful gases, including NO<sub>2</sub> and SO<sub>2</sub>, due to their strong adsorbing characteristics, wide surface area, and high reaction capacity (157-160).

#### 5.7.1. Dye removal

2,4-Dichlorophenol (2,4-DCP) is a hazardous substance that is often discharged from paper companies into various water sources, functioning as a main effluent in water. This chlorophenol compound (2,4-DCP) is known to have negative effects on people, animals, and plants who consume it, but treatment with MgO NPs has resulted in its rapid degradation because magnesium oxide acts as a catalyst in the degradation of this dye through the ionization Technique (161).

Acid Red 73 dye, a water contaminant released in large quantities from the textile industry, was removed by S. Jorfi *et al.*, and B.J.H. Ng *et al.* showed that the activity of ferrate VI, which oxidizes the Blue 203 dye (a water-contaminating dye from the leather and cosmetic industries), is enhanced by MgO NPs (162). Numerous other industries, like the fabric and clothing sectors, employ a variety of dyes to color clothing, with indigo carmine, a water effluent, being one of the most often used ones. MgO NPs were created by A. Bagheri GH *et al.* and used

as a photocatalyst for the photocatalytic decolorization of indigo carmine(163).

#### 5.7.2. Heavy metal ion removal and detection

MgO NPs have been shown by Y. Cai *et al.* to be a novel possibility for the removal of heavy metals like lead (Pb<sup>2+</sup>) and cadmium (Cd<sup>2+</sup>)(164). Nanocomposites such as magnesium oxide-copper oxide nanocomposites and magnesium oxide-manganese oxide nanocomposites, which compete with other nanoparticles involved in the removal of heavy metals from water, are effective adsorbents and have demonstrated high adsorbing properties towards heavy metal ions such as lead, arsenic, and mercury(165).

Improved MgO NPs' sensitivity, By demonstrating the exceptional detection of heavy metals like nickel, copper, and cadmium that are present in significant concentrations in well water, tap water, as well as seawater, these nanoparticles, when modified with graphene oxide, demonstrate (166).

#### 5.7.3. Chemical toxin detection and elimination

Magnesium oxide nanoparticles' ability to act as detoxifying agents is widely exploited in many different contexts, one of which is the identification and elimination of chemical pollutants. When treated with MgO NPs, the highly toxic chemical bis(2-chloroethyl) sulfide, also known as sulfur mustard and typically used as a biological warfare agent, can be broken down into non-harmful products like divinyl sulfide, thiodiglycol, and 2-chloroethyl vinyl sulfide, which are the byproducts of elimination and nucleophilic substitution reactions, respectively (167). According to S. Ali *et al.*, 2,4,6-trinitrophenyl, a very hazardous pollutant known to induce tumors, liver malfunctions, skin-related problems, etc., is degraded in MgO NPs, and ZnO NPs(168).

#### 5.7.4. degradation of pesticides and hydrogen peroxide sensors

Although pesticides serve to increase agricultural productivity by preventing pests and insects from destroying crops, when these chemicals leak from the field into other water sources, they cause several dangerous illnesses to both plants and people. According to L.E. Lange *et al.*, etching MgO NPs combined with polypropylene improves the chemical stability of the reactive sites present in the nanoparticles that break down methyl parathion, an organophosphate insecticide (169). Aluminum oxide and MgO NPs have been discovered to reduce the harmful effects of the diazinon herbicide, which the Environmental Protection Agency has prohibited due to its high toxicity toward both plants and people(170).

Hydrogen peroxide, a consequence of highly selective oxidative processes, has numerous important uses in a wide range of industries and disciplines, including medicinal, therapeutic, environmental, agricultural, industrial, and many more. As a result, its identification by a sensitive and precise approach is required(171). MgO NPs, an inorganic substance, and chitosan, an organic polymer, are used to create biosensor devices for the

detection of hydrogen peroxide(172). Nanosensors are created for the detection of hydrogen peroxide in milk using magnesium oxide nanoparticles. The created nano biosensor is inexpensive, quick, and very sensitive, able to pick up even the tiniest amount of H<sub>2</sub>O<sub>2</sub> (173).

Despite the numerous uses for MgO NPs already mentioned, there are still many more. For example, very small amounts of these particles are sufficient to improve the ability of polyurethane films to resist

corrosion, and these particles, along with nanofiltration membranes, can remove pollutants like nitrogen species, organic matter, bacteria, heavy metals, and suspended solid particles to make water safe for drinking(174). Due to their unique qualities, such as high recovery and repeatability, electrostatic, attraction abrasiveness, and oxidizing power, which work together to increase biocidal capabilities, these nanoparticles have become widely used in wastewater treatment in Figure 6 (175).

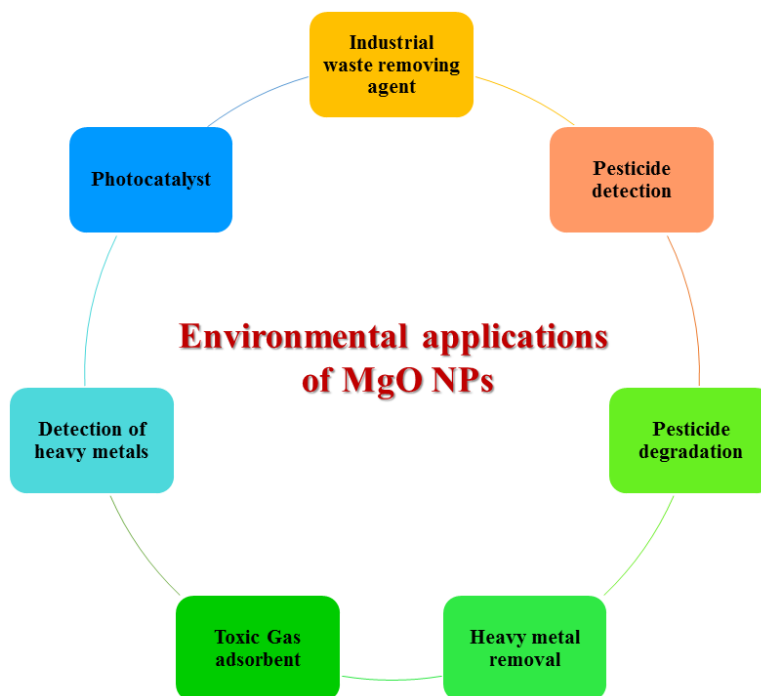


**Figure 6:** Environmental applications for MgO NPs.

## 6. CONCLUSION

Physical, chemical, and biological approaches to the synthesis of MgONPs are surveyed in the present review. Chemical and physical methods typically utilize toxic materials and are related to high energy consumption. Biological methods are currently being advocated by researchers due to their simplicity, cost-effectiveness, and environmental friendliness. Therefore, it is important to put a greater emphasis on more widespread greener methods to produce MgONPs, since this activity will be associated to some extent with the reduction of environmental pollution. MgONPs have various industrial applications, which can change energy production and protect crops from diseases caused by plant pathogens. The major problem of nanostructured MgO, as synthesized using different routes, is the occurrence of a wide band gap. Therefore, there is a crucial need to develop the synthesis method that will enable obtaining MgONPs of a narrow bandgap, making a much wider industrial application of this nanomaterial.

## 7. CONFLICT OF INTEREST

The authors possessed no relevant financial or non-financial interests.

## 8. ACKNOWLEDGMENTS

Funding open access charges: Universidade de Vigo/CISUG.

## 9. REFERENCES

1. Silva GA. Introduction to nanotechnology and its applications to medicine. *Surg Neurol* [Internet]. 2004 Mar 1;61(3):216–20. Available from: [<URL>](#).
2. Zeghoud S, Hemmami H, Ben Seghir B, Ben Amor I, Kouadri I, Rebiai A, et al. A review on biogenic green synthesis of ZnO nanoparticles by plant biomass and their applications. *Mater Today Commun* [Internet]. 2022 Dec 1;33:104747. Available from: [<URL>](#).
3. Yang W, Peters JI, Williams RO. Inhaled nanoparticles—A current review. *Int J Pharm* [Internet]. 2008 May 22;356(1–2):239–47. Available from: [<URL>](#).
4. Buzea C, Pacheco II, Robbie K. Nanomaterials and nanoparticles: Sources and toxicity. *Biointerphases* [Internet]. 2007 Dec 1;2(4):MR17–71. Available from: [<URL>](#).
5. Imani MM, Safaei M. Optimized Synthesis of Magnesium Oxide Nanoparticles as Bactericidal

- Agents. *J Nanotechnol* [Internet]. 2019 Apr 1;2019:6063832. Available from: [<URL>](#).
6. Ben Amor I, Emran TB, Hemmami H, Zeghoud S, Laouini SE. Nanomaterials based on chitosan for skin regeneration: an update. *Int J Surg* [Internet]. 2023 Mar 1;109(3):594–6. Available from: [<URL>](#).
7. Tang ZX, Lv BF. MgO nanoparticles as antibacterial agent: preparation and activity. *Brazilian J Chem Eng* [Internet]. 2014 Sep 1;31(3):591–601. Available from: [<URL>](#).
8. Sirota V, Selemenev V, Kovaleva M, Pavlenko I, Mamunin K, Dokalov V, et al. Synthesis of Magnesium Oxide Nanopowder by Thermal Plasma Using Magnesium Nitrate Hexahydrate. *Phys Res Int* [Internet]. 2016 Feb 17;2016:6853405. Available from: [<URL>](#).
9. Krishnamoorthy K, Moon JY, Hyun HB, Cho SK, Kim SJ. Mechanistic investigation on the toxicity of MgO nanoparticles toward cancer cells. *J Mater Chem* [Internet]. 2012 Nov 13;22(47):24610–7. Available from: [<URL>](#).
10. Anu Mary Ealia S, Saravanakumar MP. A review on the classification, characterisation, synthesis of nanoparticles and their application. *IOP Conf Ser Mater Sci Eng* [Internet]. 2017 Nov 1;263(3):032019. Available from: [<URL>](#).
11. Haldorai Y, Shim JJ. An efficient removal of methyl orange dye from aqueous solution by adsorption onto chitosan/MgO composite: A novel reusable adsorbent. *Appl Surf Sci* [Internet]. 2014 Feb 15;292:447–53. Available from: [<URL>](#).
12. Ngô C, Van de Voorde M. *Nanotechnology in a Nutshell* [Internet]. Paris: Atlantis Press; 2014. Available from: [<URL>](#).
13. Feng SH, Li GH. Hydrothermal and Solvothermal Syntheses. In: Ruren X, Yan X, editors. *Modern Inorganic Synthetic Chemistry* [Internet]. Elsevier; 2017. p. 73–104. Available from: [<URL>](#).
14. Sakka S. *Handbook of Sol-gel Science and Technology, Processing Characterization and Applications. Volume 1 Sol-Gel Processing*. Dordrecht, Netherlands: Kluwer Academic Publishers; 2005.
15. Rane AV, Kanny K, Abitha VK, Thomas S. Methods for Synthesis of Nanoparticles and Fabrication of Nanocomposites. In: *Synthesis of Inorganic Nanomaterials* [Internet]. Elsevier; 2018. p. 121–39. Available from: [<URL>](#).
16. Sereni JGR. Reference module in materials science and materials engineering. 2016;
17. Pal G, Rai P, Pandey A. Green synthesis of nanoparticles: A greener approach for a cleaner future. In: Kumar Shukla A, Irvani S, editors. *Green Synthesis, Characterization and Applications of Nanoparticles* [Internet]. Elsevier; 2019. p. 1–26. Available from: [<URL>](#).
18. Escudero A, Carrillo-Carrión C, Romero-Ben E, Franco A, Rosales-Barrios C, Castillejos MC, et al. Molecular Bottom-Up Approaches for the Synthesis of Inorganic and Hybrid Nanostructures. *Inorganics* [Internet]. 2021 Jul 17;9(7):58. Available from: [<URL>](#).
19. Soytas SH, Oğuz O, Menceloğlu YZ. Polymer Nanocomposites With Decorated Metal Oxides. In: Pielichowski K, Majka TM, editors. *Polymer Composites with Functionalized Nanoparticles* [Internet]. Elsevier; 2019. p. 287–323. Available from: [<URL>](#).
20. Danks AE, Hall SR, Schnepf Z. The evolution of 'sol-gel' chemistry as a technique for materials synthesis. *Mater Horizons* [Internet]. 2016 Feb 29;3(2):91–112. Available from: [<URL>](#).
21. Mastuli MS, Ansari NS, Nawawi MA, Mahat AM. Effects of Cationic Surfactant in Sol-gel Synthesis of Nano Sized Magnesium Oxide. *APCBEE Procedia* [Internet]. 2012 Jan 1;3:93–8. Available from: [<URL>](#).
22. Sutapa IW, Wahid Wahab A, Taba P, Nafie NL. Dislocation, crystallite size distribution and lattice strain of magnesium oxide nanoparticles. *J Phys Conf Ser* [Internet]. 2018 Mar 1;979(1):012021. Available from: [<URL>](#).
23. Wahab R, Ansari SG, Dar MA, Kim YS, Shin HS. Synthesis of Magnesium Oxide Nanoparticles by Sol-Gel Process. *Mater Sci Forum* [Internet]. 2007 Oct;558–559:983–6. Available from: [<URL>](#).
24. Boddu VM, Viswanath DS, Maloney SW. Synthesis and Characterization of Coralline Magnesium Oxide Nanoparticles. *J Am Ceram Soc* [Internet]. 2008 May 6;91(5):1718–20. Available from: [<URL>](#).
25. Dercz G, Prusik K, Pająk L, Pielaszek R, Malinowski JJ, Pudło W. Structure studies on nanocrystalline powder of MgO xerogel prepared by sol-gel method. *Mater Sci* [Internet]. 2009;27(1):201–7. Available from: [<URL>](#).
26. Rani N, Chahal S, Chauhan AS, Kumar P, Shukla R, Singh SK. X-ray Analysis of MgO Nanoparticles by Modified Scherer's Williamson-Hall and Size-Strain Method. *Mater Today Proc* [Internet]. 2019 Jan 1;12(3):543–8. Available from: [<URL>](#).
27. Nassar MY, Mohamed TY, Ahmed IS, Samir I. MgO nanostructure via a sol-gel combustion synthesis method using different fuels: An efficient nano-adsorbent for the removal of some anionic textile dyes. *J Mol Liq* [Internet]. 2017 Jan 1;225:730–40. Available from: [<URL>](#).
28. Mantzaris N V. Liquid-phase synthesis of nanoparticles: Particle size distribution dynamics and control. *Chem Eng Sci* [Internet]. 2005 Sep 1;60(17):4749–70. Available from: [<URL>](#).
29. Swihart MT. Vapor-phase synthesis of nanoparticles. *Curr Opin Colloid Interface Sci*

- [Internet]. 2003 Mar 1;8(1):127–33. Available from: [<URL>](#).
30. Benrabaa R, Boukhlof H, Bordes-Richard E, Vannier RN, Barama A. Nanosized nickel ferrite catalysts for CO<sub>2</sub> reforming of methane at low temperature: effect of preparation method and acid-base properties. In: *Studies in Surface Science and Catalysis* [Internet]. Elsevier; 2010. p. 301–4. Available from: [<URL>](#).
31. Huang G, Lu CH, Yang HH. Magnetic Nanomaterials for Magnetic Bioanalysis. In: Wang X, Chen X, editors. *Novel Nanomaterials for Biomedical, Environmental and Energy Applications* [Internet]. Elsevier; 2019. p. 89–109. Available from: [<URL>](#).
32. Hornak J. Synthesis, Properties, and Selected Technical Applications of Magnesium Oxide Nanoparticles: A Review. *Int J Mol Sci* [Internet]. 2021 Nov 25;22(23):12752. Available from: [<URL>](#).
33. Tartaj P, Morales M a del P, Veintemillas-Verdaguer S, Gonzalez-Carre o T, Serna CJ. The preparation of magnetic nanoparticles for applications in biomedicine. *J Phys D Appl Phys* [Internet]. 2003 Jul 7;36(13):R182–97. Available from: [<URL>](#).
34. Alaei M, Jalali M, Alimorad A. Simple and Economical Method for the Preparation of MgO Nanostructures with Suitable Surface Area. *J Chem Chem Eng* [Internet]. 2014;33(1):21–8. Available from: [<URL>](#).
35. Kumar R, Sharma A, Kishore N. Preparation and Characterization of MgO Nanoparticles by Co-Precipitation Method. *Int J Chem Phys Astron* [Internet]. 2016 Sep;70:33–41. Available from: [<URL>](#).
36. Karthikeyan V, Dhanapandian S, Manoharan C. Characterization and Antibacterial Behavior of MgO-PEG Nanoparticles Synthesized via Co-Precipitation Method. *Int Lett Chem Phys Astron* [Internet]. 2016 Sep;70:33–41. Available from: [<URL>](#).
37. Frantina YI, Fajaroh F, Nazriati, Yahmin, Sumari. Synthesis of MgO/CoFe<sub>2</sub>O<sub>4</sub> nanoparticles with coprecipitation method and its characterization. In: *AIP Conference Proceedings* [Internet]. American Institute of Physics Inc.; 2021. p. 070003. Available from: [<URL>](#).
38. Kushwaha A, Bagchi T. MgO NPs synthesis, capping and enhanced free radical effect on the bacteria and its cell morphology. In: *AIP Conference Proceedings* [Internet]. American Institute of Physics Inc.; 2018. p. 030010. Available from: [<URL>](#).
39. Varma A, Mukasyan AS, Rogachev AS, Manukyan K V. Solution Combustion Synthesis of Nanoscale Materials. *Chem Rev* [Internet]. 2016 Dec 14;116(23):14493–586. Available from: [<URL>](#).
40. Mukasyan AS, Manukyan KV. One- and Two-Dimensional Nanostructures Prepared by Combustion Synthesis. In: Pottathara YB, editor. *Nanomaterials Synthesis* [Internet]. Elsevier; 2019. p. 85–120. Available from: [<URL>](#).
41. Stojanovic BD, Dzunuzovic AS, Ilic NI. Review of methods for the preparation of magnetic metal oxides. In: Stojanovic BD, editor. *Magnetic, Ferroelectric, and Multiferroic Metal Oxides* [Internet]. Elsevier; 2018. p. 333–59. Available from: [<URL>](#).
42. Mukasyan AS, Dinka P. Novel approaches to solution-combustion synthesis of nanomaterials. *Int J Self-Propagating High-Temperature Synth* [Internet]. 2007 Mar;16(1):23–35. Available from: [<URL>](#).
43. Balakrishnan G, Velavan R, Mujasam Batoo K, Raslan EH. Microstructure, optical and photocatalytic properties of MgO nanoparticles. *Results Phys* [Internet]. 2020 Mar 1;16:103013. Available from: [<URL>](#).
44. Rao KV, Sunandana CS. Structure and microstructure of combustion synthesized MgO nanoparticles and nanocrystalline MgO thin films synthesized by solution growth route. *J Mater Sci* [Internet]. 2008 Jan 29;43(1):146–54. Available from: [<URL>](#).
45. Ranjan A, Dawn SS, Jayaprabakar J, Nirmala N, Saikiran K, Sai Sriram S. Experimental investigation on effect of MgO nanoparticles on cold flow properties, performance, emission and combustion characteristics of waste cooking oil biodiesel. *Fuel* [Internet]. 2018 May 15;220:780–91. Available from: [<URL>](#).
46. Tharani K, Jegatha Christy A, Sagadevan S, Nehru LC. Fabrication of Magnesium oxide nanoparticles using combustion method for a biological and environmental cause. *Chem Phys Lett* [Internet]. 2021 Jan 16;763:138216. Available from: [<URL>](#).
47. Kumar D, Yadav LSR, Lingaraju K, Manjunath K, Suresh D, Prasad D, et al. Combustion synthesis of MgO nanoparticles using plant extract: Structural characterization and photoluminescence studies. In: *AIP Conference Proceedings* [Internet]. American Institute of Physics Inc.; 2015. p. 050145. Available from: [<URL>](#).
48. Ng JJ, Leong KH, Sim LC, Oh WD, Dai C, Saravanan P. Environmental remediation using nano-photocatalyst under visible light irradiation: the case of bismuth phosphate. In: *Nanomaterials for Air Remediation* [Internet]. Elsevier; 2020. p. 193–207. Available from: [<URL>](#).
49. Williams MJ, Corr SA. Magnetic Nanoparticles for Targeted Cancer Diagnosis and Therapy. In: Summers H, editor. *Nanomedicine* [Internet]. Amsterdam, Netherlands: Elsevier; 2013. Available from: [<URL>](#).
50. Chircov C, Grumezescu AM, Holban AM. Magnetic Particles for Advanced Molecular Diagnosis. *Materials (Basel)* [Internet]. 2019 Jul 5;12(13):2158. Available from: [<URL>](#).
51. Devaraja PB, Avadhani DN, Prashantha SC, Nagabhushana H, Sharma SC, Nagabhushana BM, et

- al. Synthesis, structural and luminescence studies of magnesium oxide nanopowder. *Spectrochim Acta Part A Mol Biomol Spectrosc* [Internet]. 2014 Jan 24;118:847–51. Available from: [<URL>](#).
52. Al-Hazmi F, Alnowaiser F, Al-Ghamdi AA, Al-Ghamdi AA, Aly MM, Al-Tuwirqi RM, et al. A new large – Scale synthesis of magnesium oxide nanowires: Structural and antibacterial properties. *Superlattices Microstruct* [Internet]. 2012 Aug 1;52(2):200–9. Available from: [<URL>](#).
53. Ding Y, Zhang G, Wu H, Hai B, Wang L, Qian Y. Nanoscale Magnesium Hydroxide and Magnesium Oxide Powders: Control over Size, Shape, and Structure via Hydrothermal Synthesis. *Chem Mater* [Internet]. 2001 Feb 1;13(2):435–40. Available from: [<URL>](#).
54. Rukh S, Sofi AH, Shah MA, Yousuf S. Antibacterial activity of magnesium oxide nanostructures prepared by hydrothermal method. *Asian J Nanosci Mater* [Internet]. 1999 Nov 30;2(4):425–30. Available from: [<URL>](#).
55. Jeevanandam J, Chan YS, Danquah MK. Biosynthesis and characterization of MgO nanoparticles from plant extracts via induced molecular nucleation. *New J Chem* [Internet]. 2017 Mar 27;41(7):2800–14. Available from: [<URL>](#).
56. Das RK, Pachapur VL, Lonappan L, Naghdi M, Pulicharla R, Maiti S, et al. Biological synthesis of metallic nanoparticles: plants, animals and microbial aspects. *Nanotechnol Environ Eng* [Internet]. 2017 Dec 9;2(1):18. Available from: [<URL>](#).
57. Ali MI, Sharma G, Kumar M, Dut Jasuja N. Biological approach of magnesium oxide nanoparticles synthesized by *Spirulina platensis*. *World J Pharm Res* [Internet]. 2015;4(7):1234–41. Available from: [<URL>](#).
58. Awwad AM, Ahmad AL. Biosynthesis, characterization, and optical properties of magnesium hydroxide and oxide nanoflakes using Citrus limon leaf extract. *Arab J Phys Chem*. 2014;1(2):66.
59. Bandeira M, Giovanela M, Roesch-Ely M, Devine DM, da Silva Crespo J. Green synthesis of zinc oxide nanoparticles: A review of the synthesis methodology and mechanism of formation. *Sustain Chem Pharm* [Internet]. 2020 Mar 1;15:100223. Available from: [<URL>](#).
60. Das B, Moumita S, Ghosh S, Khan MI, Indira D, Jayabalan R, et al. Biosynthesis of magnesium oxide (MgO) nanoflakes by using leaf extract of *Bauhinia purpurea* and evaluation of its antibacterial property against *Staphylococcus aureus*. *Mater Sci Eng C* [Internet]. 2018 Oct 1;91:436–44. Available from: [<URL>](#).
61. Jadhav AH, Lim AC, Thorat GM, Jadhav HS, Seo JG. Green solvent ionic liquids: structural directing pioneers for microwave-assisted synthesis of controlled MgO nanostructures. *RSC Adv* [Internet]. 2016 Mar 29;6(38):31675–86. Available from: [<URL>](#).
62. Singh A, Joshi NC, Ramola M. Magnesium oxide Nanoparticles (MgONPs): Green Synthesis, Characterizations and Antimicrobial activity. *Res J Pharm Technol* [Internet]. 2019 Oct 1;12(10):4644–6. Available from: [<URL>](#).
63. Cai L, Liu M, Liu Z, Yang H, Sun X, Chen J, et al. MgONPs Can Boost Plant Growth: Evidence from Increased Seedling Growth, Morpho-Physiological Activities, and Mg Uptake in Tobacco (*Nicotiana tabacum* L.). *Molecules* [Internet]. 2018 Dec 19;23(12):3375. Available from: [<URL>](#).
64. Wrigglesworth EG, Johnston JH. Mie theory and the dichroic effect for spherical gold nanoparticles: an experimental approach. *Nanoscale Adv* [Internet]. 2021 Jun 15;3(12):3530–6. Available from: [<URL>](#).
65. El-Seedi HR, El-Shabasy RM, Khalifa SAM, Saeed A, Shah A, Shah R, et al. Metal nanoparticles fabricated by green chemistry using natural extracts: biosynthesis, mechanisms, and applications. *RSC Adv* [Internet]. 2019 Aug 8;9(42):24539–59. Available from: [<URL>](#).
66. Khan MI, Akhtar MN, Ashraf N, Najeeb J, Munir H, Awan TI, et al. Green synthesis of magnesium oxide nanoparticles using *Dalbergia sissoo* extract for photocatalytic activity and antibacterial efficacy. *Appl Nanosci* [Internet]. 2020 Jul 25;10(7):2351–64. Available from: [<URL>](#).
67. Duong THY, Nguyen TN, Oanh HT, Dang Thi TA, Giang LNT, Phuong HT, et al. Synthesis of Magnesium Oxide Nanoplates and Their Application in Nitrogen Dioxide and Sulfur Dioxide Adsorption. *J Chem* [Internet]. 2019 May 26;2019:4376429. Available from: [<URL>](#).
68. Yuvakkumar R, Hong SI. Green Synthesis of Spinel Magnetite Iron Oxide Nanoparticles. *Adv Mater Res* [Internet]. 2014 Oct 27;1051:39–42. Available from: [<URL>](#).
69. Vergheese M, Vishal Sk, Mary Vergheese C. Green synthesis of magnesium oxide nanoparticles using *Trigonella foenum-graecum* leaf extract and its antibacterial activity. *J Pharmacogn Phytochem* [Internet]. 2018;7(3):1193–200. Available from: [<URL>](#).
70. Younis IY, El-Hawary SS, Eldahshan OA, Abdel-Aziz MM, Ali ZY. Green synthesis of magnesium nanoparticles mediated from *Rosa floribunda* charisma extract and its antioxidant, antiaging and antibiofilm activities. *Sci Rep* [Internet]. 2021 Aug 19;11(1):16868. Available from: [<URL>](#).
71. Abdallah Y, Ogunyemi SO, Abdelazez A, Zhang M, Hong X, Ibrahim E, et al. The Green Synthesis of MgO Nano-Flowers Using *Rosmarinus officinalis* L. (Rosemary) and the Antibacterial Activities against *Xanthomonas oryzae* pv. *oryzae*. *Biomed Res Int* [Internet]. 2019 Feb 17;2019:5620989. Available from: [<URL>](#).

72. Amina M, Al Musayeib NM, Alarfaj NA, El-Tohamy MF, Oraby HF, Al Hamoud GA, et al. Biogenic green synthesis of MgO nanoparticles using *Saussurea costus* biomasses for a comprehensive detection of their antimicrobial, cytotoxicity against MCF-7 breast cancer cells and photocatalysis potentials. Mishra YK, editor. *PLoS One* [Internet]. 2020 Aug 14;15(8):e0237567. Available from: [<URL>](#).
73. Sharma G, Soni R, Jasuja ND. Phytoassisted synthesis of magnesium oxide nanoparticles with *Swertia chirayaita*. *J Taibah Univ Sci* [Internet]. 2017 May 16;11(3):471–7. Available from: [<URL>](#).
74. Fatiqin A, Amrulloh H, Simanjuntak W. Green synthesis of MgO nanoparticles using *Moringa oleifera* leaf aqueous extract for antibacterial activity. *Bull Chem Soc Ethiop* [Internet]. 2021 May 7;35(1):161–70. Available from: [<URL>](#).
75. Nguyen DTC, Dang HH, Vo DVN, Bach LG, Nguyen TD, Tran T Van. Biogenic synthesis of MgO nanoparticles from different extracts (flower, bark, leaf) of *Tecoma stans* (L.) and their utilization in selected organic dyes treatment. *J Hazard Mater* [Internet]. 2021 Feb 15;404:124146. Available from: [<URL>](#).
76. Suresh J, Yuvakkumar R, Sundrarajan M, Hong SI. Green Synthesis of Magnesium Oxide Nanoparticles. *Adv Mater Res* [Internet]. 2014 May;952:141–4. Available from: [<URL>](#).
77. Narendhran S, Manikandan M, Shakila PB. Antibacterial, antioxidant properties of *Solanum trilobatum* and sodium hydroxide-mediated magnesium oxide nanoparticles: a green chemistry approach. *Bull Mater Sci* [Internet]. 2019 Jun 25;42(3):133. Available from: [<URL>](#).
78. Rahmani-Nezhad S, Dianat S, Saedi M, Hadjiakhoondi A. Characterization and Catalytic Activity of Plant-Mediated MgO Nanoparticles Using *Mucuna Pruriens* L. Seed Extract and Their Biological Evaluation. *J Nanoanalysis* [Internet]. 2017;4(4):290–8. Available from: [<URL>](#).
79. Prasanth R, Kumar SD, Jayalakshmi A, Singaravelu G, Govindaraju K, Kumar VG. Green synthesis of magnesium oxide nanoparticles and their antibacterial activity. *IJMS Vol48(08)* [August 2019] [Internet]. 2019;48(08):1210–5. Available from: [<URL>](#).
80. Anantharaman A, Sathyabhama S, George M. Green synthesis of magnesium oxide nanoparticles using *Aloe Vera* and its applications. *IJSRD—International J Sci Res Dev*. 2016;4(9):20.
81. Abinaya S, Kavitha HP, Prakash M. Sustainable Chemistry and Pharmacy.
82. Jhansi K, Jayarambabu N, Reddy KP, Reddy NM, Suvarna RP, Rao KV, et al. Biosynthesis of MgO nanoparticles using mushroom extract: effect on peanut (*Arachis hypogaea* L.) seed germination. *3Biotech* [Internet]. 2017 Aug 25;7(4):263. Available from: [<URL>](#).
83. Raliya R, Tarafdar JC, Choudhary K, Mal P, Raturi A, Gautam R, et al. Synthesis of MgO Nanoparticles Using *Aspergillus Tubingensis* TFR-3. *J Bionanoscience* [Internet]. 2014 Feb 1;8(1):34–8. Available from: [<URL>](#).
84. Ibrahim E, Thalij K, Badawy A. Antibacterial Potential of Magnesium Oxide Nanoparticles Synthesized by *Aspergillus niger*. *Biotechnol J Int* [Internet]. 2017 Jan 10;18(1):1–7. Available from: [<URL>](#).
85. Mohanasrinivasan V, Subathra Devi C, Mehra A, Prakash S, Agarwal A, Selvarajan E, et al. Biosynthesis of MgO Nanoparticles Using *Lactobacillus* Sp. and its Activity Against Human Leukemia Cell Lines HL-60. *Bionanoscience* [Internet]. 2018 Mar 5;8(1):249–53. Available from: [<URL>](#).
86. Kaul RK, Kumar P, Burman U, Joshi P, Agrawal A, Raliya R, et al. Magnesium and iron nanoparticles production using microorganisms and various salts. *Mater Sci* [Internet]. 2012 Sep 14;30(3):254–8. Available from: [<URL>](#).
87. Essien ER, Atasié VN, Okefor AO, Nwude DO. Biogenic synthesis of magnesium oxide nanoparticles using *Manihot esculenta* (Crantz) leaf extract. *Int Nano Lett* [Internet]. 2020 Mar 23;10(1):43–8. Available from: [<URL>](#).
88. Pugazhendhi A, Prabhu R, Muruganantham K, Shanmuganathan R, Natarajan S. Anticancer, antimicrobial and photocatalytic activities of green synthesized magnesium oxide nanoparticles (MgONPs) using aqueous extract of *Sargassum wightii*. *J Photochem Photobiol B Biol* [Internet]. 2019 Jan 1;190:86–97. Available from: [<URL>](#).
89. Dobrucka R. Synthesis of MgO Nanoparticles Using *Artemisia abrotanum* Herba Extract and Their Antioxidant and Photocatalytic Properties. *Iran J Sci Technol Trans A Sci* [Internet]. 2018 Jun 2;42(2):547–55. Available from: [<URL>](#).
90. Ghidan AY, Al-Antary TM, Awwad AM. Green synthesis of magnesium oxide (MgONPs) nanoparticles using *Chamaemel umnobile* flowers extract: Effect on Green Peach Aphid. In: *The 3rd International Nanotechnology Conference and Expo Italy Madridge Journal Nanotechnology Science*. 2018. p. 67.
91. Subhan MA, Chandra Saha P, Uddin N, Sarker P. Synthesis, Structure, Spectroscopy and Photocatalytic Studies of Nano Multi-Metal Oxide MgO·Al<sub>2</sub>O<sub>3</sub>·ZnO and MgO·Al<sub>2</sub>O<sub>3</sub>·ZnO·Curcumin Composite. *Int J Nanosci Nanotechnol* [Internet]. 2017 Feb 1;13(1):69–82. Available from: [<URL>](#).
92. Srivastava V, Sharma YC, Sillanpää M. Green synthesis of magnesium oxide nanoflower and its application for the removal of divalent metallic species from synthetic wastewater. *Ceram Int* [Internet]. 2015 Jun 1;41(5):6702–9. Available from: [<URL>](#).

93. Sugirtha P, Divya R, Yedhukrishnan R, Suganthi KS, Anusha N, Ponnusami V, et al. Green Synthesis of Magnesium Oxide Nanoparticles Using Brassica oleracea and Punica granatum Peels and their Anticancer and Photocatalytic Activity. *Asian J Chem* [Internet]. 2015 Jul 1;27(7):2513–7. Available from: [<URL>](#).
94. Munjal S, Singh A, Kumar V. Synthesis and characterization of MgO nanoparticles by orange fruit waste through green method. *Int J Adv Res Comput Sci*. 2017;4(9):36–42.
95. Kumara KNS, Nagaswarupa HP, Mahesh KR V, Mylarappa M, Prashantha SC, Siddeshwara DMK, et al. Synthesis and characterization of ZnO/MgO nano particles by curry leaves through green approach and their photocatalytic applications. *Int J Adv Res*. 2016;4(10):1958–62.
96. Umaralikhhan L, Jamal Mohamed Jaffar M. Green Synthesis of MgO Nanoparticles and its Antibacterial Activity. *Iran J Sci Technol Trans A Sci* [Internet]. 2018 Jun 7;42(2):477–85. Available from: [<URL>](#).
97. Anantharama NA, Sheethal KS, Mary G. Green synthesis and its applications of magnesium oxide nanoparticles from the seeds of lepidium sativum. *Int J Recent Sci Res*. 2016;7:14029–32.
98. Ogunyemi SO, Zhang F, Abdallah Y, Zhang M, Wang Y, Sun G, et al. Biosynthesis and characterization of magnesium oxide and manganese dioxide nanoparticles using *Matricaria chamomilla* L. extract and its inhibitory effect on *Acidovorax oryzae* strain RS-2. *Artif Cells, Nanomedicine, Biotechnol* [Internet]. 2019 Dec 4;47(1):2230–9. Available from: [<URL>](#).
99. Yildirim M, Akarsu H. Preparation of magnesium oxide (MgO) from dolomite by leach-precipitation-pyrohydrolysis process. *Physicochem Probl Miner Process* [Internet]. 2010;44:257–72. Available from: [<URL>](#).
100. Mustafa AMK, Al-Dahan DK, Khachik T V. Laboratory study of MgO preparation from Iraqi dolomite by leach-precipitation-pyrohydrolysis process. *Iraqi Bull Geol Min*. 2014;10(3):83–107.
101. Kulikova SA, Vinokurov SE, Khamizov RK, Vlasovskikh NS, Belova KY, Dzheloda RK, et al. The Use of MgO Obtained from Serpentine in the Synthesis of a Magnesium Potassium Phosphate Matrix for Radioactive Waste Immobilization. *Appl Sci* [Internet]. 2020 Dec 28;11(1):220. Available from: [<URL>](#).
102. Mantilaka MMMGPG, Pitawala HMTGA, Karunaratne DGGP, Rajapakse RMG. Nanocrystalline magnesium oxide from dolomite via poly(acrylate) stabilized magnesium hydroxide colloids. *Colloids Surfaces A Physicochem Eng Asp* [Internet]. 2014 Feb 20;443:201–8. Available from: [<URL>](#).
103. Jassim AK, Salmtori SA, Jassam JA. Sustainable manufacturing process applied to produce magnesium oxide from sea water. *IOP Conf Ser Mater Sci Eng* [Internet]. 2020 Mar 1;757(1):012021. Available from: [<URL>](#).
104. Sirota V, Selemenev V, Kovaleva M, Pavlenko I, Mamunin K, Dokalov V, et al. Preparation of crystalline Mg(OH)<sub>2</sub> nanopowder from serpentine mineral. *Int J Min Sci Technol* [Internet]. 2018 May 1;28(3):499–503. Available from: [<URL>](#).
105. Chen Y, Yang X, Wu L, Tong L, Zhu J. Recovery of Mg from H<sub>2</sub>SO<sub>4</sub> Leaching Solution of Serpentine to Precipitation of High-Purity Mg(OH)<sub>2</sub> and 4MgCO<sub>3</sub>·Mg(OH)<sub>2</sub>·4H<sub>2</sub>O. *Minerals* [Internet]. 2023 Feb 23;13(3):318. Available from: [<URL>](#).
106. Ben Amor I, Hemmami H, Laouini SE, Mahboub MS, Barhoum A. Sol-Gel Synthesis of ZnO Nanoparticles Using Different Chitosan Sources: Effects on Antibacterial Activity and Photocatalytic Degradation of AZO Dye. *Catalysts* [Internet]. 2022 Dec 8;12(12):1611. Available from: [<URL>](#).
107. Ben Amor I, Hemmami H, Laouini SE, Abdelaziz AG, Barhoum A. Influence of chitosan source and degree of deacetylation on antibacterial activity and adsorption of AZO dye from water. *Biomass Convers Biorefinery* [Internet]. 2023 Jan 11;1:1–11. Available from: [<URL>](#).
108. Diachenko OV, Opanasuyk AS, Kurbatov DI, Opanasuyk NM, Kononov OK, Nam D, et al. Surface Morphology, Structural and Optical Properties of MgO Films Obtained by Spray Pyrolysis Technique. *Acta Phys Pol A* [Internet]. 2016 Sep;130(3):805–10. Available from: [<URL>](#).
109. Alexander L, Klug HP. Determination of Crystallite Size with the X-Ray Spectrometer. *J Appl Phys* [Internet]. 1950 Feb 1;21(2):137–42. Available from: [<URL>](#).
110. Holzwarth U, Gibson N. The Scherrer equation versus the “Debye-Scherrer equation”. *Nat Nanotechnol* [Internet]. 2011 Aug 28;6(9):534. Available from: [<URL>](#).
111. Al-Tabbakh AA, Karatepe N, Al-Zubaidi AB, Benchaabane A, Mahmood NB. Crystallite size and lattice strain of lithiated spinel material for rechargeable battery by X-ray diffraction peak-broadening analysis. *Int J Energy Res* [Internet]. 2019 Apr 1;43(5):1903–11. Available from: [<URL>](#).
112. Kimiagar S, Abrinaei F. Effect of temperature on the structural, linear, and nonlinear optical properties of MgO-doped graphene oxide nanocomposites. *Nanophotonics* [Internet]. 2018 Jan 26;7(1):243–51. Available from: [<URL>](#).
113. Verma R, Naik KK, Gangwar J, Srivastava AK. Morphology, mechanism and optical properties of nanometer-sized MgO synthesized via facile wet chemical method. *Mater Chem Phys* [Internet]. 2014 Dec 15;148(3):1064–70. Available from: [<URL>](#).
114. Li J, Khalid A, Verma R, Abraham A, Qazi F, Dong X, et al. Silk Fibroin Coated Magnesium Oxide Nanospheres: A Biocompatible and Biodegradable Tool for Noninvasive Bioimaging Applications.

- Nanomaterials [Internet]. 2021 Mar 10;11(3):695. Available from: [<URL>](#).
115. Ben Amor I, Hemmami H, Laouini SE, Temam H Ben, Zaoui H, Barhoum A. Biosynthesis MgO and ZnO nanoparticles using chitosan extracted from *Pimelia Payraudi Latreille* for antibacterial applications. *World J Microbiol Biotechnol* [Internet]. 2023 Jan 21;39(1):19. Available from: [<URL>](#).
116. Yarbrough R, Davis K, Dawood S, Rathnayake H. A sol-gel synthesis to prepare size and shape-controlled mesoporous nanostructures of binary (II-VI) metal oxides. *RSC Adv* [Internet]. 2020 Apr 6;10(24):14134-46. Available from: [<URL>](#).
117. Sainudeen SS, Asok LB, Varghese A, Nair AS, Krishnan G. Surfactant-driven direct synthesis of a hierarchical hollow MgO nanofiber-nanoparticle composite by electrospinning. *RSC Adv* [Internet]. 2017 Jul 13;7(56):35160-8. Available from: [<URL>](#).
118. Guo Y, Hu J, Wan L. Nanostructured Materials for Electrochemical Energy Conversion and Storage Devices. *Adv Mater* [Internet]. 2008 Aug 4;20(15):2878-87. Available from: [<URL>](#).
119. Sayle DC, Seal S, Wang Z, Mangili BC, Price DW, Karakoti AS, et al. Mapping Nanostructure: A Systematic Enumeration of Nanomaterials by Assembling Nanobuilding Blocks at Crystallographic Positions. *ACS Nano* [Internet]. 2008 Jun 1;2(6):1237-51. Available from: [<URL>](#).
120. Stark J V., Park DG, Lagadic I, Klabunde KJ. Nanoscale Metal Oxide Particles/Clusters as Chemical Reagents. Unique Surface Chemistry on Magnesium Oxide As Shown by Enhanced Adsorption of Acid Gases (Sulfur Dioxide and Carbon Dioxide) and Pressure Dependence. *Chem Mater* [Internet]. 1996 Jan 1;8(8):1904-12. Available from: [<URL>](#).
121. Sutradhar N, Sinhamahapatra A, Pahari SK, Pal P, Bajaj HC, Mukhopadhyay I, et al. Controlled Synthesis of Different Morphologies of MgO and Their Use as Solid Base Catalysts. *J Phys Chem C* [Internet]. 2011 Jun 30;115(25):12308-16. Available from: [<URL>](#).
122. Dobrucka R. Synthesis of MgO Nanoparticles Using *Artemisia abrotanum* Herba Extract and Their Antioxidant and Photocatalytic Properties. *Iran J Sci Technol Trans A Sci* [Internet]. 2018 Jun 2;42(2):547-55. Available from: [<URL>](#).
123. Sheng O, Jin C, Luo J, Yuan H, Huang H, Gan Y, et al. Mg<sub>2</sub>B<sub>2</sub>O<sub>5</sub> Nanowire Enabled Multifunctional Solid-State Electrolytes with High Ionic Conductivity, Excellent Mechanical Properties, and Flame-Retardant Performance. *Nano Lett* [Internet]. 2018 May 9;18(5):3104-12. Available from: [<URL>](#).
124. Shao Y, Rajput NN, Hu J, Hu M, Liu T, Wei Z, et al. Nanocomposite polymer electrolyte for rechargeable magnesium batteries. *Nano Energy* [Internet]. 2015 Mar 1;12:750-9. Available from: [<URL>](#).
125. Sun W, Sun X, Peng Q, Wang H, Ge Y, Akhtar N, et al. Nano-MgO/AB decorated separator to suppress shuttle effect of lithium-sulfur battery. *Nanoscale Adv* [Internet]. 2019 Apr 9;1(4):1589-97. Available from: [<URL>](#).
126. Zhang R, Tutusaus O, Mohtadi R, Ling C. Magnesium-Sodium Hybrid Battery With High Voltage, Capacity and Cyclability. *Front Chem* [Internet]. 2018 Dec 10;6:611. Available from: [<URL>](#).
127. Saha P, Datta MK, Velikokhatnyi OI, Manivannan A, Alman D, Kumta PN. Rechargeable magnesium battery: Current status and key challenges for the future. *Prog Mater Sci* [Internet]. 2014 Oct 1;66:1-86. Available from: [<URL>](#).
128. Wang J, Wang C, Gong S, Chen Q. Enhancing the Capacitance of Battery-Type Hybrid Capacitors by Encapsulating MgO Nanoparticles in Porous Carbon as Reservoirs for OH<sup>-</sup> Ions from Electrolytes. *ACS Appl Mater Interfaces* [Internet]. 2019 Jun 19;11(24):21567-77. Available from: [<URL>](#).
129. Julkapli NM, Bagheri S. Magnesium oxide as a heterogeneous catalyst support. *Rev Inorg Chem* [Internet]. 2016 Jan 1;36(1):1-41. Available from: [<URL>](#).
130. Scarsella M, de Caprariis B, Damizia M, De Filippis P. Heterogeneous catalysts for hydrothermal liquefaction of lignocellulosic biomass: A review. *Biomass and Bioenergy* [Internet]. 2020 Sep 1;140:105662. Available from: [<URL>](#).
131. Almerindo GI, Probst LFD, Campos CEM, de Almeida RM, Meneghetti SMP, Meneghetti MR, et al. Magnesium oxide prepared via metal-chitosan complexation method: Application as catalyst for transesterification of soybean oil and catalyst deactivation studies. *J Power Sources* [Internet]. 2011 Oct 1;196(19):8057-63. Available from: [<URL>](#).
132. Vickers NJ. Animal Communication: When I'm Calling You, Will You Answer Too? *Curr Biol* [Internet]. 2017 Jul 24;27(14):R713-5. Available from: [<URL>](#).
133. Kantam ML, Pal U, Sreedhar B, Choudary BM. An Efficient Synthesis of Organic Carbonates using Nanocrystalline Magnesium Oxide. *Adv Synth Catal* [Internet]. 2007 Jul 2;349(10):1671-5. Available from: [<URL>](#).
134. Yang XF, Zhang MJ, Hou XL, Dai LX. Stereocontrolled Aziridination of Imines via a Sulfonium Ylide Route and a Mechanistic Study. *J Org Chem* [Internet]. 2002 Nov 1;67(23):8097-103. Available from: [<URL>](#).
135. Mastuli MS, Kamarulzaman N, Nawawi MA, Mahat AM, Rusdi R, Kamarudin N. Growth mechanisms of MgO nanocrystals via a sol-gel synthesis using different complexing agents. *Nanoscale Res Lett* [Internet]. 2014 Dec 21;9(1):134. Available from: [<URL>](#).

136. Kumar D, Reddy VB, Mishra BG, Rana RK, Nadagouda MN, Varma RS. Nanosized magnesium oxide as catalyst for the rapid and green synthesis of substituted 2-amino-2-chromenes. *Tetrahedron* [Internet]. 2007 Apr 9;63(15):3093–7. Available from: [<URL>](#).
137. Kantam ML, Chakrapani L, Ramani T. Synthesis of  $\alpha$ -diazo- $\beta$ -hydroxy esters using nanocrystalline MgO. *Tetrahedron Lett* [Internet]. 2007 Aug 27;48(35):6121–3. Available from: [<URL>](#).
138. Chintareddy VR, Lakshmi Kantam M. Recent Developments on Catalytic Applications of Nano-Crystalline Magnesium Oxide. *Catal Surv from Asia* [Internet]. 2011 Jun 19;15(2):89–110. Available from: [<URL>](#).
139. Singh RP. Application of Nanomaterials Toward Development of Nanobiosensors and Their Utility in Agriculture. In: *Nanotechnology* [Internet]. Singapore: Springer Singapore; 2017. p. 293–303. Available from: [<URL>](#).
140. Khot LR, Sankaran S, Maja JM, Ehsani R, Schuster EW. Applications of nanomaterials in agricultural production and crop protection: A review. *Crop Prot* [Internet]. 2012 May 1;35:64–70. Available from: [<URL>](#).
141. Singh RP. Utility of Nanomaterials in Food Safety. In: *Food Safety and Human Health* [Internet]. Elsevier; 2019. p. 285–318. Available from: [<URL>](#).
142. Rao Kandregula G, Rao KG, Ashok CH, Rao KV, Chakra CS. Structural properties of MgO Nanoparticles: Synthesized by Co-Precipitation Technique. *Int J Sci Res ISSN* [Internet]. 2014;3(12):43–6. Available from: [<URL>](#).
143. Al-Noaman A, Rawlinson SCF, Hill RG. The role of MgO on thermal properties, structure and bioactivity of bioactive glass coating for dental implants. *J Non Cryst Solids* [Internet]. 2012 Nov 1;358(22):3019–27. Available from: [<URL>](#).
144. Boys AJ, McCorry MC, Rodeo S, Bonassar LJ, Estroff LA. Next generation tissue engineering of orthopedic soft tissue-to-bone interfaces. *MRS Commun* [Internet]. 2017 Sep 3;7(3):289–308. Available from: [<URL>](#).
145. Fahmy HM, El-Hakim MH, Nady DS, Elkaramany Y, Mohamed FA, Yasien AM, et al. Review on MgO nanoparticles multifunctional role in the biomedical field: Properties and applications. *Nanomedicine J* [Internet]. 2022 Jan 1;9(1):1–14. Available from: [<URL>](#).
146. He Y, Ingudam S, Reed S, Gehring A, Strobaugh TP, Irwin P. Study on the mechanism of antibacterial action of magnesium oxide nanoparticles against foodborne pathogens. *J Nanobiotechnology* [Internet]. 2016 Dec 27;14(1):54. Available from: [<URL>](#).
147. Cai L, Chen J, Liu Z, Wang H, Yang H, Ding W. Magnesium Oxide Nanoparticles: Effective Agricultural Antibacterial Agent Against *Ralstonia solanacearum*. *Front Microbiol* [Internet]. 2018 Apr 25;9:335574. Available from: [<URL>](#).
148. Ibrahim E, Fouad H, Zhang M, Zhang Y, Qiu W, Yan C, et al. Biosynthesis of silver nanoparticles using endophytic bacteria and their role in inhibition of rice pathogenic bacteria and plant growth promotion. *RSC Adv* [Internet]. 2019 Sep 17;9(50):29293–9. Available from: [<URL>](#).
149. Abdallah ESH, Mahmoud MM, Abdel-Rahim IR. *Trichosporon jirovecii* infection of red swamp crayfish (*Procambarus clarkii*). *J Fish Dis* [Internet]. 2018 Nov 26;41(11):1719–32. Available from: [<URL>](#).
150. Huber DM, Jones JB. The role of magnesium in plant disease. *Plant Soil* [Internet]. 2013 Jul 11;368(1–2):73–85. Available from: [<URL>](#).
151. Wang WN, Tarafdar JC, Biswas P. Nanoparticle synthesis and delivery by an aerosol route for watermelon plant foliar uptake. *J Nanoparticle Res* [Internet]. 2013 Jan 10;15(1):1417. Available from: [<URL>](#).
152. Chen J, Peng H, Wang X, Shao F, Yuan Z, Han H. Graphene oxide exhibits broad-spectrum antimicrobial activity against bacterial phytopathogens and fungal conidia by intertwining and membrane perturbation. *Nanoscale* [Internet]. 2014 Jan 16;6(3):1879–89. Available from: [<URL>](#).
153. Kumar K, Sridhar J, Choudhary VK, Singh HK, Parameshwari B, Senthil Kumar KM, et al. New Innovations and Approaches for Biotic Stress Management of Crops. In: *Ghost PK, Kumar P, Chakraborty D, Mandal D, Sivalingam PN, editors. Innovations in Agriculture for a Self-Reliant India* [Internet]. London: CRC Press; 2021. p. 265–92. Available from: [<URL>](#).
154. Rao W, Zhan Y, Chen S, Xu Z, Huang T, Hong X, et al. Flowerlike Mg(OH)<sub>2</sub> Cross-Nanosheets for Controlling Cry1Ac Protein Loss: Evaluation of Insecticidal Activity and Biosecurity. *J Agric Food Chem* [Internet]. 2018 Apr 11;66(14):3651–7. Available from: [<URL>](#).
155. Imada K, Sakai S, Kajihara H, Tanaka S, Ito S. Magnesium oxide nanoparticles induce systemic resistance in tomato against bacterial wilt disease. *Plant Pathol* [Internet]. 2016 May 18;65(4):551–60. Available from: [<URL>](#).
156. Radzig MA, Nadtochenko VA, Koksharova OA, Kiwi J, Lipasova VA, Khmel IA. Antibacterial effects of silver nanoparticles on gram-negative bacteria: Influence on the growth and biofilms formation, mechanisms of action. *Colloids Surfaces B Biointerfaces* [Internet]. 2013 Feb 1;102:300–6. Available from: [<URL>](#).
157. Wang T, Liu X, Zhao D, Jiang Z. The unusual electrochemical characteristics of a novel three-dimensional ordered bicontinuous mesoporous carbon. *Chem Phys Lett* [Internet]. 2004 May 11;389(4–6):327–31. Available from: [<URL>](#).

158. Camtakan Z, Erenturk S (Akyil), Yusan S (Doyurum). Magnesium oxide nanoparticles: Preparation, characterization, and uranium sorption properties. *Environ Prog Sustain Energy* [Internet]. 2012 Dec 15;31(4):536–43. Available from: [<URL>](#).
159. Park JY, Lee YJ, Jun KW, Baeg JO, Yim DJ. Chemical Synthesis and Characterization of Highly Oil Dispersed MgO Nanoparticles. *J Ind Eng Chem* [Internet]. 2006;12(6):882–7. Available from: [<URL>](#).
160. Štengl V, Bakardjieva S, Maříková M, Bezdička P, Šubrt J. Magnesium oxide nanoparticles prepared by ultrasound enhanced hydrolysis of Mg-alkoxides. *Mater Lett* [Internet]. 2003 Aug 1;57(24–25):3998–4003. Available from: [<URL>](#).
161. Mohammadi L, Bazrafshan E, Noroozifar M, Ansari-Moghaddam A, Barahuie F, Balarak D. Removing 2,4-dichlorophenol from aqueous environments by heterogeneous catalytic ozonation using synthesized MgO nanoparticles. *Water Sci Technol* [Internet]. 2017 Dec 6;76(11):3054–68. Available from: [<URL>](#).
162. Tara N, Siddiqui SI, Rathi G, Chaudhry SA, Inamuddin, Asiri AM. Nano-engineered Adsorbent for the Removal of Dyes from Water: A Review. *Curr Anal Chem* [Internet]. 2020 Jan 8;16(1):14–40. Available from: [<URL>](#).
163. Bagheri GH A, Sabbaghan M, Mirgani Z. A comparative study on properties of synthesized MgO with different templates. *Spectrochim Acta Part A Mol Biomol Spectrosc* [Internet]. 2015 Feb 25;137:1286–91. Available from: [<URL>](#).
164. Wu D, Bai Y, Wang W, Xia H, Tan F, Zhang S, et al. Highly pure MgO<sub>2</sub> nanoparticles as robust solid oxidant for enhanced Fenton-like degradation of organic contaminants. *J Hazard Mater* [Internet]. 2019 Jul 15;374:319–28. Available from: [<URL>](#).
165. Askari P, Faraji A, Khayatian G, Mohebbi S. Effective ultrasound-assisted removal of heavy metal ions As(III), Hg(II), and Pb(II) from aqueous solution by new MgO/CuO and MgO/MnO<sub>2</sub> nanocomposites. *J Iran Chem Soc* [Internet]. 2017 Mar 2;14(3):613–21. Available from: [<URL>](#).
166. Khayatian G, Jodan M, Hassanpoor S, Mohebbi S. Determination of trace amounts of cadmium, copper and nickel in environmental water and food samples using GO/MgO nanocomposite as a new sorbent. *J Iran Chem Soc* [Internet]. 2016 May 21;13(5):831–9. Available from: [<URL>](#).
167. Štengl V, Maříková M, Bakardjieva S, Šubrt J, Opluštil F, Olšanská M. Reaction of sulfur mustard gas, soman and agent VX with nanosized anatase TiO<sub>2</sub> and ferrihydrite. *J Chem Technol Biotechnol* [Internet]. 2005 Jul 14;80(7):754–8. Available from: [<URL>](#).
168. Ali S, Farrukh MA, Khaleeq-ur-Rahman M. Photodegradation of 2,4,6-trinitrophenol catalyzed by Zn/MgO nanoparticles prepared in aqueous-organic medium. *Korean J Chem Eng* [Internet]. 2013 Nov 6;30(11):2100–7. Available from: [<URL>](#).
169. Lange LE, Obendorf SK. Effect of Plasma Etching on Destructive Adsorption Properties of Polypropylene Fibers Containing Magnesium Oxide Nanoparticles. *Arch Environ Contam Toxicol* [Internet]. 2012 Feb 18;62(2):185–94. Available from: [<URL>](#).
170. Behnam R, Morshed M, Tavanai H, Ghiaci M. Destructive Adsorption of Diazinon Pesticide by Activated Carbon Nanofibers Containing Al<sub>2</sub>O<sub>3</sub> and MgO Nanoparticles. *Bull Environ Contam Toxicol* [Internet]. 2013 Oct 4;91(4):475–80. Available from: [<URL>](#).
171. Singh RP, Tiwari A, Pandey AC. Silver/Polyaniline Nanocomposite for the Electrocatalytic Hydrazine Oxidation. *J Inorg Organomet Polym Mater* [Internet]. 2011 Dec 13;21(4):788–92. Available from: [<URL>](#).
172. Lu L, Zhang L, Zhang X, Wu Z, Huan S, Shen G, et al. A MgO Nanoparticles Composite Matrix-Based Electrochemical Biosensor for Hydrogen Peroxide with High Sensitivity. *Electroanalysis* [Internet]. 2010 Feb 4;22(4):471–7. Available from: [<URL>](#).
173. Dong X xiu, Li M ying, Feng N nan, Sun Y ming, Yang C, Xu Z lin. A nanoporous MgO based nonenzymatic electrochemical sensor for rapid screening of hydrogen peroxide in milk. *RSC Adv* [Internet]. 2015 Oct 13;5(105):86485–9. Available from: [<URL>](#).
174. An Y, Zhang K, Wang F, Lin L, Guo H. Removal of organic matters and bacteria by nano-MgO/GAC system. *Desalination* [Internet]. 2011 Oct 17;281(1):30–4. Available from: [<URL>](#).
175. Ramanujam K, Sundrarajan M. Biocidal activities of monochlorotriazine-β-cyclodextrine with MgO modified cellulosic fabrics. *J Text Inst* [Internet]. 2015 Nov 2;106(11):1147–53. Available from: [<URL>](#).